526 *J. Phys. Chem. A* **2007,** *111,* 526−540

Computational Study of the Reactions of SiH_3X (X = H, Cl, Br, I) with HCN

Shahidul M. Islam, Joshua W. Hollett, and Raymond A. Poirier*

Department of Chemistry, Memorial University of Newfoundland, St. John's, Newfoundland, Canada A1B 3X7

Received: October 4, 2006; In Final Form: November 6, 2006

Ab initio calculations were carried out for the reactions of silane and halosilanes (SiH_3X, X = H, Cl, Br, I) with HCN. Geometries of the reactants, transition states, intermediates and products were optimized at HF, MP2, and B3LYP levels of theory using the 6-31G(d) and 6-31G(d,p) basis sets. Energies were also obtained using G3MP2 and G3B3 levels of theory. Intrinsic reaction coordinate (IRC) calculations were performed to characterize the transition states on the potential energy surface. It was found that HCN can react with silane and halosilanes via three different mechanisms. One involves HX elimination by a one-step pathway producing SiH_3CN. The second mechanism consists of H_2 elimination, producing SiH_2XCN via a one-step pathway or three multiple-step pathways. The third mechanism involves dissociation of SiH_3X to various products, which can then react with HCN. Activation energies, enthalpies, and free energies of activation along with the thermodynamic properties (ΔE, ΔH, and ΔG) of each reaction pathway were calculated. The reaction of SiH_3X with HCN produce different products depending on substituent X. We have found that the standard 6-31G(d) bromine basis set gave results which were in better agreement with the G3MP2 results than for the Binning−Curtiss basis set. Computed heats of formation (ΔH_f) for SiH_3CN, SiH_3NC, SiH_2ClCN, SiH_2BrCN, SiH_2ICN, SiHCl, SiHBr, and SiHI were found to be 133.5, 150.8, −34.4, 23.6, 102.4, 48.7, 127.1, and 179.8 kJ mol^{-1}, respectively. From enthalpies calculated at G3MP2, we predict that the ΔH_f for SiH_2 to be 262.8 kJ mol^{-1} compared to the experimental value of 273.8 ± 4.2 kJ mol^{-1}.

1. Introduction

In recent years, silanes (SiH_4) and halosilanes (SiH_3X) have drawn considerable attention because of their importance in the semiconductor, glass, and polymer industries.[1−4] The physical and chemical properties of most silyl compounds are quite different from those of their methyl analogues. Although silicon and carbon are isovalent, silicon can have co-ordinations greater than four. Silicon also interacts with the π-bonds of elements in groups V, VI, and VII. Unlike carbon, silicon does not favor formation of multiple bonds. Silane and halosilanes can react with small molecules, such as NH_3[5] and H_2O,[6] to form various intermediates and products under suitable conditions. Similar reactions may be possible in interstellar space where Si is relatively abundant.[7] As a consequence, a number of researchers have focused on the reactions of silane and halosilanes, both experimentally and theoretically.[7−14]

The gas-phase reactions of silane with ammonia and water were studied using ab initio methods by Hu et al.[5,6] The reaction with NH_3 was found to proceed in a single step to the most stable product silylamine (SiH_3NH_2). The reaction involves H_2 elimination from the weakly bonded reactant complex H_3N/SiH_4. The activation energy was found to be 206.1 kJ mol^{-1} at the CCSD(T)/6-311++G(d,p)//MP2/6-31+G(d) level. This barrier was the lowest among various pathways investigated for the reaction. For the gas-phase reaction between SiH_4 and H_2O, 40 equilibrium and 27 transition state structures were found on the potential energy surface of the reaction. The reaction, $SiH_4 + H_2O \rightarrow SiH_3OH + H_2$ has an energy barrier of 194.8 kJ mol^{-1} and ΔE_{rxn} of −45.3 kJ mol^{-1} at CCSD(T)/6-311++G-(d,p)//MP2/6-31+G(d). It was found that SiH_4/H_2O can also eliminate H_2 to produce SiH_2/H_2O with an energy barrier of 242.8 kJ mol^{-1}. The products can further eliminate H_2 or H, producing smaller molecules SiHOH, $SiH_2{-}O$, $Si{-}H_2O$, and SiO, and $SiH_2{-}OH$, $SiH{-}H_2O$, HSiO, and HOSi radicals.

Silanes have been found both experimentally and theoretically to complex with the lone-paired electrons of ammonia, amine, arsine, phosphorus or phosphine to form pentacoordinated adducts.[15−21] Feng et al.[22] investigated the adducts H_3SiX/NH_3 (X = F, Cl, Br, I) with ab initio calculations at the G2MP2 level, and discussed the influence of halogen atoms on the structure and stability of this type of species. Schlegel et al.[23,24] studied the thermal decomposition of SiH_4 and SiH_3Cl at HF/6-31G(d) and MP2/6-31G(d,p). They found that for the decomposition of SiH_4, $SiH_2 + H_2$ is favored over SiH_3 + H and for SiH_3C1, SiHCl + H_2 is preferred over SiH_2 + HCl. Calculations have also shown that in the gas phase, SiH_4 and Ga in its first excited ^2S state, react to form SiH_3 radicals, H atoms, GaH and $GaSiH_3$.[25]

The number of known Si-containing molecules is very small compared to C or N containing species and few compounds containing all three are known. In interstellar space, only the simplest radicals, SiCN and SiNC, have been detected.[26] In the laboratory, HSiCN and HSiNC[27] have been detected, along with the SiCN and SiNC[28] radicals. More hydrogenated species H_3CNSi, H_3SiCN, and H_3SiNC were also characterized by IR spectra.[29] A G3B3 investigation of the singlet [H_3, Si, N, C] isomers[30] resulted in 26 isomers and 45 interconversion transition state structures. The three lowest-lying isomers, H_3SiCN (0.0 kJ mol^{-1}), H_3SiNC (20.5 kJ mol^{-1}), and H_3CNSi (30.9 kJ mol^{-1}) were found to be kinetically stable with the lowest conversion barrier at 98.0 kJ mol^{-1}. Fourteen new isomers with considerable kinetic stability were also predicted. To date, no

---

* Corresponding author. Telephone: (709) 737-8609. Fax: (709) 737-3702. E-mail: rpoirier@mun.ca.

10.1021/jp066524o CCC: $37.00

TABLE 1: Activation Energies and Free Energies of Activation for the Reaction of SiH_3X (X = H, Cl, Br, I) with HCN (HX Elimination) and the Isomerization of SiH_3CN/HX (in kJ mol^{-1}) at 298.15 K (Pathway A)[a,b]

		HX elimination		isomerization	
X	level/basis set	$\Delta E_{a,TS1}{}^{A}$	$\Delta G^{\ddagger}{}_{TS1}{}^{A}$	$\Delta E_{a,TS2}{}^{A}$	$\Delta G^{\ddagger}{}_{TS2}{}^{A}$
H	HF/6-31G(d)	374.7	387.6	127.7	122.2
	HF/6-31G(d,p)	353.3	367.1	127.8	121.9
	MP2/6-31G(d)	332.1	342.8	134.6	134.6
	MP2/6-31G(d,p)	311.5	322.3	133.9	138.4
	B3LYP/6-31G(d)	305.3	315.0	123.7	122.4
	B3LYP/6-31G(d,p)	290.3	300.9	123.8	122.9
	G3MP2	280.7	296.4	115.1	114.6
	G3B3	279.6	294.6	119.1	113.4
Cl	HF/6-31G(d)	376.0	368.5	137.5	125.8
	HF/6-31G(d,p)	360.5	348.3	137.5	121.1
	MP2/6-31G(d)	315.6	310.9	142.9	137.4
	MP2/6-31G(d,p)	295.8	291.7	141.5	136.3
	B3LYP/6-31G(d)	273.9	280.7	132.4	115.3
	B3LYP/6-31G(d,p)	264.3	266.4	131.8	115.5
	G3MP2	265.5	264.3	121.2	116.7
	G3B3	269.7	262.0	125.9	115.0
Br	HF/6-31G(d)	374.5 (373.9)	373.0 (367.8)	135.9 (131.1)	128.0 (127.8)
	HF/6-31G(d,p)	364.6 (364.0)	363.4 (347.0)	136.0 (131.1)	128.5 (128.1)
	MP2/6-31G(d)	306.7 (312.8)	310.7 (309.5)	142.0 (137.3)	137.4 (137.9)
	MP2/6-31G(d,p)	295.4 (300.3)	298.6 (290.6)	140.7 (135.7)	136.3 (136.2)
	B3LYP/6-31G(d)	265.8 (274.7)	269.5 (279.8)	131.1 (127.7)	127.9 (128.7)
	B3LYP/6-31G(d,p)	260.1 (267.0)	264.6 (264.8)	130.8 (124.0)	127.9 (121.6)
	G3MP2	261.1 (271.2)	275.9 (283.5)	119.7 (120.1)	117.1 (121.7)
I	MP2/6-31G(d)	302.8	320.4	140.4	139.2
	MP2/6-31G(d,p)	297.3	301.1	139.1	137.7
	B3LYP/6-31G(d)	259.7	289.3	129.3	121.6
	B3LYP/6-31G(d,p)	256.0	275.0	129.1	128.9

[a] Mechanistic pathway and barriers as defined in Figure 1 and 2, respectively. [b] The values in parentheses are calculated by using the Binning−Curtiss bromine basis set from ref 39.

TABLE 2: Activation Energies and Free Energies of Activation for the Reaction of SiH_3X (X = H, Cl, Br, I) with HCN (in kJ mol^{-1}) at 298.15 K (H_2 Elimination: Pathways B1, B*, and B2)[c]

		pathway B1[a]		pathway B*[a]				pathway B2[b]	
X	level/basis set	$\Delta E_{a,TS1}{}^{B1}$	$\Delta G^{\ddagger}{}_{TS1}{}^{B1}$	$\Delta E_{a,TS1}{}^{B*}$	$\Delta G^{\ddagger}{}_{TS1}{}^{B*}$	$\Delta E_{a,TS2}{}^{B*}$	$\Delta G^{\ddagger}{}_{TS2}{}^{B*}$	$\Delta E_{a,TS1}{}^{B2}$	$\Delta G^{\ddagger}{}_{TS1}{}^{B2}$
H	HF/6-31G(d)	374.7	387.6	392.1	362.5	129.7	122.6	385.2	400.7
	HF/6-31G(d,p)	353.3	367.1	364.3	337.1	129.8	122.5	299.2	321.1
	MP2/6-31G(d)	332.1	342.8	317.9	291.5	92.2	87.9	336.4	353.1
	MP2/6-31G(d,p)	311.5	322.3	293.1	268.2	92.3	87.6	334.5	350.9
	B3LYP/6-31G(d)	305.3	315.0	313.6	286.8	99.4	97.0	271.0	287.0
	B3LYP/6-31G(d,p)	290.3	300.9	293.1	268.1	99.5	94.5	270.2	286.4
	G3MP2	280.7	296.4	262.3	261.6	97.3	94.6	265.4	283.8
	G3B3	279.6	294.6	267.6	266.9	97.2	99.1	272.1	290.3
Cl	HF/6-31G(d)	363.9	368.5	392.6	364.6	142.0	134.1	358.6	366.8
	HF/6-31G(d,p)	342.3	348.3	364.7	338.9	142.0	133.7	355.6	364.7
	MP2/6-31G(d)	306.1	310.9	315.2	290.6	102.2	97.4	310.4	320.1
	MP2/6-31G(d,p)	286.4	291.7	290.2	267.0	102.5	97.2	308.6	318.7
	B3LYP/6-31G(d)	277.7	280.7	308.7	283.7	110.0	106.2	241.8	250.6
	B3LYP/6-31G(d,p)	262.7	266.4	288.3	265.1	110.1	106.1	240.0	249.0
	G3MP2	252.8	264.3	258.7	258.6	107.2	103.8	236.6	250.1
	G3B3	251.8	262.0	264.8	264.8	107.2	110.7	242.7	255.0
Br	HF/6-31G(d)	368.2 (363.5)	373.1 (367.8)	391.2 (392.6)	363.7 (364.2)	141.4 (140.4)	133.5 (132.7)	361.7 (360.6)	370.4 (368.7)
	HF/6-31G(d,p)	346.6 (341.9)	352.2 (347.0)	363.5 (364.9)	338.0 (338.6)	141.6 (140.6)	133.2 (132.4)	358.6 (357.6)	367.6 (366.0)
	MP2/6-31G(d)	309.9 (306.2)	313.8 (309.5)	312.4 (313.4)	288.6 (288.9)	101.0 (100.3)	96.6 (95.8)	311.9 (310.8)	320.9 (319.1)
	MP2/6-31G(d,p)	290.0 (286.5)	294.7 (290.6)	287.5 (288.6)	265.1 (265.6)	101.3 (100.6)	96.3 (95.2)	310.2 (309.1)	319.8 (318.1)
	B3LYP/6-31G(d)	281.4 (277.7)	283.7 (279.8)	306.0 (308.3)	282.0 (282.8)	109.0 (108.5)	105.6 (104.6)	244.2 (243.4)	252.5 (251.4)
	B3LYP/6-31G(d,p)	266.2 (262.6)	268.9 (264.8)	285.7 (288.0)	263.6 (264.3)	109.2 (108.6)	104.8 (104.2)	242.4 (241.7)	250.8 (249.4)
	G3MP2	256.1 (256.3)	267.6 (267.3)	256.4 (256.4)	256.7 (255.9)	106.2 (106.2)	102.7 (103.0)	239.0 (238.9)	252.5 (251.8)
I	MP2/6-31G(d)	316.9	320.4	325.4	300.4	99.2	94.8	314.2	323.2
	MP2/6-31G(d,p)	296.8	301.1	299.9	276.1	99.4	94.3	312.6	322.3
	B3LYP/6-31G(d)	287.3	289.3	317.5	291.8	107.3	102.2	247.5	256.1
	B3LYP/6-31G(d,p)	272.0	275.0	297.4	273.3	107.4	101.8	245.8	254.9

[a] Mechanistic pathway and barriers as defined in Figure 3 and 5, respectively. [b] Mechanistic pathway and barriers as defined in Figure 4 and 6, respectively. [c] The values in parentheses are calculated by using the Binning−Curtiss bromine basis set from ref 39.

experimental or theoretical heats of formation have been reported for H_3SiCN and H_3SiNC.

No computational studies have been reported for the reaction of silanes and halosilanes with HCN. To ensure the reliability of our results, wave function and DFT calculations were performed. One of the main objectives of this study was to select the lowest level of theory/basis set that would give reliable energetics for these reactions. Because of the size of the system,

TABLE 3: Activation Energies and Free Energies of Activation for the Reaction of SiH_3X (X = H, Cl, Br, I) with HCN (in kJ mol^{-1}) at 298.15 K (H_2 Elimination: Pathways B3 and B4)[a,d]

		pathway B3[b]						pathway B4[c]			
X	level/basis set	$\Delta E_{\mathrm{a,TS1}}^{\mathrm{B3}}$	$\Delta G^{\ddagger}{}_{\mathbf{TS1}}^{\mathrm{B3}}$	$\Delta E_{\mathrm{a,TS2}}^{\mathrm{B3}}$	$\Delta G^{\ddagger}{}_{\mathbf{TS2}}^{\mathrm{B3}}$	$\Delta E_{\mathrm{a,TS3}}^{\mathrm{B3}}$	$\Delta G^{\ddagger}{}_{\mathbf{TS3}}^{\mathrm{B3}}$	$\Delta E_{\mathrm{a,TS1}}^{\mathrm{B4}}$	$\Delta G^{\ddagger}{}_{\mathbf{TS1}}^{\mathrm{B4}}$	$\Delta E_{\mathrm{a,TS2}}^{\mathrm{B4}}$	$\Delta G^{\ddagger}{}_{\mathbf{TS2}}^{\mathrm{B4}}$
Cl	HF/6-31G(d)	387.7	394.8	9.0	11.9	173.5	162.7	381.7	387.9	−5.6	−3.1
	B3LYP/6-31G(d)	272.2	280.7	7.9	11.3	190.2	180.3	268.6	276.7	−3.9	−1.2
	B3LYP/6-31G(d,p)	269.7	278.1	7.9	11.6	189.3	179.5	266.1	274.3	−3.8	−0.8
	G3MP2	268.6	282.0	6.0	9.7	176.5	177.1	260.7	272.2	−2.3	1.4
Br	HF/6-31G(d)	390.1 (389.6)	397.9 (396.7)	9.5 (8.8)	12.5 (11.5)	173.1 (173.6)	162.4 (162.6)	383.2 (382.5)	390.0 (388.3)	6.9 (6.1)	8.8 (8.0)
	HF/6-31G(d,p)	386.5	394.5	9.6	12.7	172.0	161.3	377.4	383.1	−5.7	−2.9
	MP2/6-31G(d)	353.3	361.9	8.2	11.6	196.8	186.2	342.0	350.4	−5.9	−3.3
	MP2/6-31G(d,p)	350.4	359.7	8.1	11.5	196.1	185.2	338.1	347.2	−5.4	−2.6
	B3LYP/6-31G(d)	273.8	281.6	9.8	13.7	191.1	181.8	269.8	277.5	−1.7	1.7
	B3LYP/6-31G(d,p)	271.3 (271.2)	279.2 (278.3)	10.0 (7.8)	13.9 (11.1)	190.3 (189.1)	180.9 (179.3)	267.0 (265.9)	274.6 (272.6)	−1.4 (12.2)	2.1 (13.7)
	G3MP2	271.0 (270.9)	284.4 (283.7)	6.4 (5.3)	10.2 (8.7)	176.0 (175.9)	176.7 (176.3)	261.4 (262.0)	272.9 (272.7)	−1.5 (2.4)	1.0 (4.9)
I	HF/6-31G(d)	394.3	402.4	9.8	12.9	172.5	162.1	385.3	392.3	7.1	9.0
	B3LYP/6-31G(d,p)	274.6	283.1	11.0	8.8	190.5	180.7	268.2	276.4	31.2	32.0

[a] Mechanistic pathways as defined in Figure 4; B3LYP/6-31G(d,p) values are shown for all X, since they agree the best with G3 values. [b] Barriers as defined in Figure 7. [c] Barriers as defined in Figure 8. [d] The values in parentheses are calculated by using the Binning−Curtiss bromine basis set from ref 39.

TABLE 4: Activation Energies, Activation Enthalpies and Free Energies of Activation for the Thermal Decomposition Reaction of SiH_3X (X = H, Cl, Br, I) (in kJ mol^{-1}) at 298.15 K (Figure 9)[b]

	$SiH_4 \rightarrow SiH_2 + H_2$			$SiH_3Cl \rightarrow SiHCl + H_2$		
level/basis set	ΔE_a	$\Delta H^{\ddagger}$	$\Delta G^{\ddagger}$	ΔE_a	$\Delta H^{\ddagger}$	$\Delta G^{\ddagger}$
HF/6-31G(d)	334.7	322.7	319.8	367.4	356.0	352.9
MP2/6-31G(d)	282.7	270.7	267.8	312.9	299.8	296.7
B3LYP/6-31G(d)	256.6	244.8	241.9	281.8	268.9	265.7
G3MP2	233.1	233.2	230.3	257.6	257.8	254.7
G3B3	235.6	235.6	232.7	260.8	261.1	257.8
	250.8[a]			280.1[a]		

	$SiH_3Br \rightarrow SiHBr + H_2$			$SiH_3I \rightarrow SiHI + H_2$		
level/basis set	ΔE_a	$\Delta H^{\ddagger}$	$\Delta G^{\ddagger}$	ΔE_a	$\Delta H^{\ddagger}$	$\Delta G^{\ddagger}$
HF/6-31G(d)	361.3 (362.2)	348.7 (349.7)	345.7 (346.6)	350.2	337.9	334.9
MP2/6-31G(d)	305.0 (304.9)	292.1 (292.0)	289.0 (288.9)	294.4	281.8	278.7
B3LYP/6-31G(d)	275.9 (275.8)	263.2 (263.3)	259.9 (260.1)	267.3	254.9	251.7
G3MP2	252.3 (252.2)	252.5 (252.3)	249.4 (252.0)			

further reactions

	$SiHCl + H_2 \rightarrow SiH_2 + HCl$			$SiHBr + H_2 \rightarrow SiH_2 + HBr$		
level/basis set	ΔE_a	$\Delta H^{\ddagger}$	$\Delta G^{\ddagger}$	ΔE_a	$\Delta H^{\ddagger}$	$\Delta G^{\ddagger}$
HF/6-31G(d)	194.9	192.6	218.8	177.2 (175.6)	174.2 (172.7)	200.2 (196.4)
MP2/6-31G(d)	171.8	168.8	191.1	155.9 (154.4)	151.7 (150.5)	173.3 (170.3)
B3LYP/6-31G(d)	129.1	124.9	142.7	117.1 (117.0)	112.1 (112.5)	130.2 (131.3)
G3MP2	128.7	119.6	146.9	118.5 (119.0)	109.4 (110.0)	136.5 (134.8)
G3B3	124.4	116.9	135.0			

	$SiHI + H_2 \rightarrow SiH_2 + HI$		
level/basis set	ΔE_a	$\Delta H^{\ddagger}$	$\Delta G^{\ddagger}$
HF/6-31G(d)	162.2	157.6	183.3
MP2/6-31G(d)	144.2	138.5	160.1
B3LYP/6-31G(d)	108.7	102.6	121.6

[a] The values obtained from ref 23. [b] The values in parentheses are calculated by using the Binning−Curtiss bromine basis set from ref 39.

it is possible to perform the calculations at high levels of theory, such as the G3MP2 and G3B3 levels, which are known to give reliable energetics.[31,32]

2. Method

All the electronic structure calculations were carried out with Gaussian03,[33] except for $TS1^A$, X = Br, where the HF structure was optimized with MUNgauss.[34] The geometries of all reactants, transition states, intermediates and products were fully optimized at the HF, second-order Møller−Plesset (MP2) and B3LYP levels of theory using the 6-31G(d) and 6-31G(d,p) basis sets. From previous work,[35] it was found that the activation energies and the enthalpies of reaction calculated using Gaussian-n theories (G1, G2, G2MP2, G3, G3MP2, G3B3, and G3MP2B3) all agreed to within 10 kJ mol^{-1}. For this study, G3MP2 and G3B3 theories have been selected due to their reliability[31,32] and the fact that they provide a contrast between wave function and density functional theories. For Br, the G3MP2large basis set,[36,37] which is not yet incorporated in Gaussian03, was used for G3MP2 calculations. The standard 6-31G(d) bromine basis set[38] has been used throughout and compared with the Binning−Curtiss[39] bromine basis set available in Gaussian03. For iodine, the Huzinaga double-ζ basis set[40] was used. Frequencies were calculated for all structures

TABLE 5: Activation Energies, Enthalpies and Free Energies of Activation for the Reaction of SiHX (X = H, Cl, Br, I) with HCN (in kJ mol^{-1}) at 298.15 K (Figure 10)[a]

	$SiH_2 + HCN \rightarrow SiH_3CN$			$SiHCl + HCN \rightarrow SiH_2ClCN$		
level/basis set	ΔE_a	$\Delta H^{\ddagger}$	$\Delta G^{\ddagger}$	ΔE_a	$\Delta H^{\ddagger}$	$\Delta G^{\ddagger}$
HF/6-31G(d)	155.5	147.0	168.3	222.2	210.8	235.9
MP2/6-31G(d)	53.3	45.0	63.4	131.8	120.9	141.9
B3LYP/6-31G(d)	34.3	26.1	45.7	109.7	98.8	121.4
G3MP2	24.8	18.0	39.8	92.4	86.0	111.6
G3B3	29.3	22.7	42.6	96.3	90.2	112.9

	$SiHBr + HCN \rightarrow SiH_2BrCN$			$SiHI + HCN \rightarrow SiH_2ICN$		
level/basis set	ΔE_a	$\Delta H^{\ddagger}$	$\Delta G^{\ddagger}$	ΔE_a	$\Delta H^{\ddagger}$	$\Delta G^{\ddagger}$
HF/6-31G(d)	221.3 (215.9)	209.8 (204.5)	235.6 (229.8)	216.0	204.4	230.6
MP2/6-31G(d)	129.4 (125.0)	118.4 (114.0)	140.0 (135.6)	122.0	111.0	132.8
B3LYP/6-31G(d)	109.9 (104.6)	98.8 (93.7)	121.3 (115.5)	107.0	95.8	118.2
G3MP2	90.5 (90.2)	84.2 (83.8)	110.5 (109.6)			

[a] The values in parentheses are calculated by using the Binning−Curtiss bromine basis set from ref 39.

TABLE 6: Thermodynamic Properties for the Reaction of SiH_3X (X = H, Cl, Br, I) with HCN (in kJ mol^{-1}) at 298.15 K (HX Elimination Reaction)[d]

	$SiH_4 + HCN \rightarrow SiH_3CN + H_2$			$SiH_3Cl + HCN \rightarrow SiH_3CN + HCl$		
level/basis set	ΔE	ΔH	ΔG	ΔE	ΔH	ΔG
HF/6-31G(d)	−2.4	−13.2	−6.0	63.6	56.8	57.4
HF/6-31G(d,p)	−5.5	−16.0	−8.9	52.3	45.7	46.3
MP2/6-31G(d)	−28.4	−37.5	−30.8	60.1	54.6	54.8
MP2/6-31G(d,p)	−23.6	−32.7	−26.0	45.5	40.2	40.4
B3LYP/6-31G(d)	−15.5	−24.5	−17.5	55.8	49.7	50.2
B3LYP/6-31G(d,p)	−15.5	−24.4	−17.4	47.6	41.6	42.1
G3MP2	−35.8	−32.9	−26.2	44.4	46.3	46.5
G3B3	−33.3	−30.5	−23.7	43.8	45.6	45.9
					45.2[a]	

	$SiH_3Br + HCN \rightarrow SiH_3CN + HBr$			$SiH_3I + HCN \rightarrow SiH_3CN + HI$		
level/basis set	ΔE	ΔH	ΔG	ΔE	ΔH	ΔG
HF/6-31G(d)	58.2 (82.0)	50.1 (73.5)	50.6 (73.9)	53.1	43.5	44.1
HF/6-31G(d,p)	51.0 (71.0)	43.3 (63.2)	43.9 (63.6)	46.8	37.6	38.2
MP2/6-31G(d)	58.4 (79.6)	51.8 (72.6)	51.9 (72.6)	54.9	46.7	47.0
MP2/6-31G(d,p)	49.5 (68.7)	43.1 (62.1)	43.3 (62.2)	47.7	39.7	40.0
B3LYP/6-31G(d)	50.7 (72.1)	43.6 (64.6)	44.1 (64.9)	45.8	37.6	38.2
B3LYP/6-31G(d,p)	46.2 (63.8)	39.3 (56.8)	39.8 (57.2)	41.9	33.9	34.6
G3MP2	42.0 (40.4)	43.6 (42.0)	43.8 (42.1)			
		29.6[b]			29.8[c]	

[a] The value is calculated from ΔH_f of SiH_3Cl, HCN, SiH_3CN, and HCl given in Table 11. [b] The value is calculated from ΔH_f of SiH_3Br, HCN, SiH_3CN, and HBr given in Table 11. [c] The value is calculated from ΔH_f of SiH_3I, HCN, SiH_3CN, and HI given in Table 11. [d] The values in parentheses are calculated by using the Binning−Curtiss bromine basis set from ref 39.

to ensure the absence of imaginary frequencies in the minima and for the presence of only one imaginary frequency in the transition states. The complete reaction pathways for all the mechanisms discussed in this paper have been verified using intrinsic reaction coordinate (IRC) analysis for all transition states. Structures at the last IRC points have been optimized to positively identify the reactant and product to which each transition state is connected. Heats of formation (ΔH_f) of SiH_3CN, SiH_3NC, SiH_2ClCN, SiH_2BrCN, SiH_2ICN, SiHCl, SiHBr, and SiHI were calculated using computed enthalpies of reaction and available experimental heats of formation (ΔH_f).

3. Results and Discussions

The results for the reactions of SiH_3X (X = H, Cl, Br, I) with HCN are given in Tables 1−10, and the heats of formation of some energetically stable compounds are presented in Table 11.

3.1. Activation Energies and Free Energies of Activation for the Reaction of SiH_3X with HCN. The results for the reaction of SiH_3X (X = H, Cl, Br, I) with HCN will be discussed in the following order: (1) HX elimination, (2) H_2 elimination, and (3) reaction of HCN with SiH_3X dissociation products.

3.1.1. Reaction of SiH_3X and HCN (Pathway A). Pathway A consists of an HX elimination reaction followed by isomerization of the SiH_3CN product:

$$SiH_3X + HCN \rightarrow SiH_3CN + HX \rightarrow SiH_3NC + HX, \quad X = H, Cl, Br, \text{and } I$$

The structures of pathway A are shown in Figure 1 for the reaction of SiH_3Cl + HCN. Similar structures are also observed for the reaction of SiH_4, SiH_3Br, and SiH_3I with HCN and hence are not shown here. The relative energies of reactants, transition states, and products are shown in Figure 2. In all cases, SiH_3X and HCN react in a single-step to form SiH_3CN and HX.

The reactant complex of SiH_3X and HCN is a weak complex of the form SiH_3X−HCN except for X = H, which has the form H_4Si−NCH. The transition state ($TS1^A$) involves two bond ruptures (Si−X and H−C) and two bond formations (Si−C and H−X). In the reactant complex R^A, the Si−X bond distances for X = H, Cl, Br, and I at MP2/6-31G(d) level of theory are

TABLE 7: Relative Stabilities for the Isomerization of SiH_2XCN/SiH_2XNC(X = H, Cl, Br, I) (in kJ mol^{-1}) at 298.15 K[b]

	$SiH_3CN \rightarrow SiH_3NC$			$SiH_2ClCN \rightarrow SiH_2ClNC$		
level/basis set	Δ*E*	Δ*H*	Δ*G*	Δ*E*	Δ*H*	Δ*G*
HF/6-31G(d)	−1.8	−2.5	−3.3	−10.7	−11.7	−12.4
HF/6-31G(d,p)	−1.8	−2.5	−3.3	−10.7	−11.6	−12.4
MP2/6-31G(d)	42.7	43.3	42.9	36.4	36.8	36.4
MP2/6-31G(d,p)	41.9	42.5	42.0	35.9	36.3	35.9
B3LYP/6-31G(d)	24.9	24.5	23.8	17.3	16.8	16.2
B3LYP/6-31G(d,p)	24.9	24.6	23.9	17.3	16.8	16.2
G3MP2	16.9	17.3	16.5	9.5	9.8	9.0
G3B3	20.6 20.5[a]	20.9	20.3	13.3	13.6	13.0

	$SiH_2BrCN \rightarrow SiH_2BrNC$			$SiH_2ICN \rightarrow SiH_2INC$		
level/basis set	Δ*E*	Δ*H*	Δ*G*	Δ*E*	Δ*H*	Δ*G*
HF/6-31G(d)	−9.1 (−8.6)	−10.1 (−9.6)	−10.9 (−10.3)	−6.7	−7.7	−8.5
HF/6-31G(d,p)	−9.1 (−8.6)	−10.0 (−9.5)	−10.8 (−10.3)	−6.8	−7.7	−8.5
MP2/6-31G(d)	38.0 (38.0)	38.4 (38.4)	38.0 (38.1)	40.5	40.9	40.6
MP2/6-31G(d,p)	37.5 (37.6)	37.9 (37.9)	37.5 (37.6)	40.0	40.4	40.0
B3LYP/6-31G(d)	18.8 (19.1)	18.2 (18.5)	17.7 (18.1)	21.0	20.4	19.8
B3LYP/6-31G(d,p)	18.8 (19.1)	18.3 (18.6)	17.7 (18.1)	21.0	20.4	19.8
G3MP2	11.2 (11.4)	11.6 (11.8)	10.8 (11.1)			

[a] The values obtained from ref 30. [b] The values in parentheses are calculated by using the Binning−Curtiss bromine basis set from ref 39.

TABLE 8: Thermodynamic Properties for the Reaction of SiH_3X (X = Cl, Br, I) with HCN (H_2 Elimination Reaction) (in kJ mol^{-1}) at 298.15 K[a]

	$SiH_3Cl + HCN \rightarrow SiH_2ClCN + H_2$		
level/basis set	Δ*E*	Δ*H*	Δ*G*
HF/6-31G(d)	7.5	−4.6	0.3
HF/6-31G(d,p)	4.4	−7.4	−2.4
MP2/6-31G(d)	−24.7	−34.9	−30.5
MP2/6-31G(d,p)	−19.8	−29.9	−25.5
B3LYP/6-31G(d)	−10.3	−20.3	−15.8
B3LYP/6-31G(d,p)	−10.4	−20.3	−15.7
G3MP2	−34.4	−30.5	−26.3
G3B3	−32.0	−28.2	−23.8

	$SiH_3Br + HCN \rightarrow SiH_2BrCN + H_2$		
level/basis set	Δ*E*	Δ*H*	Δ*G*
HF/6-31G(d)	9.3 (6.4)	−2.8 (−5.8)	2.2 (−1.0)
HF/6-31G(d,p)	6.3 (3.4)	−5.5 (−8.5)	−0.5 (−3.6)
MP2/6-31G(d)	−23.2 (−25.2)	−33.3 (−35.5)	−28.9 (−31.3)
MP2/6-31G(d,p)	−18.4 (−20.3)	−28.4 (−30.5)	−24.0 (−26.2)
B3LYP/6-31G(d)	−8.9 (−11.9)	−18.9 (−22.0)	−14.3 (−17.6)
B3LYP/6-31G(d,p)	−9.0 (−11.9)	−18.8 (−21.8)	−14.3 (−17.5)
G3MP2	−33.8 (−33.9)	−29.8 (−29.9)	−25.5 (−23.0)

	$SiH_3I + HCN \rightarrow SiH_2ICN + H_2$		
level/basis set	Δ*E*	Δ*H*	Δ*G*
HF/6-31G(d)	10.8	−1.1	3.8
HF/6-31G(d,p)	7.9	−3.7	1.2
MP2/6-31G(d)	−22.0	−32.1	−27.7
MP2/6-31G(d,p)	−17.2	−27.2	−22.8
B3LYP/6-31G(d)	−8.0	−17.8	−13.2
B3LYP/6-31G(d,p)	−7.9	−17.6	−13.1

[a] The values in parentheses are calculated by using the Binning−Curtiss bromine basis set from ref 39.

1.482, 2.070, 2.242, and 2.486 Å, respectively, while in TS1^A, they increase to 1.687, 2.449, 2.726, and 3.179 Å respectively. Similarly, the C−H bond distance of 1.070 Å in R^A for X = H, Cl, Br, and I increase to 1.613, 1.455, 1.304, and 1.191 Å, respectively, in TS1^A. The intrinsic reaction coordinate (IRC) analysis confirmed that TS1^A leads to the SiH_3X/HCN and SiH_3CN/HX complexes. The activation energies for the HX elimination reaction along with the isomerization of SiH_3CN/HX to SiH_3NC/HX are listed in Table 1. The activation energies ($\Delta E_{a,TS1}{}^{A}$) and free energies of activation($\Delta G^{\ddagger}_{TS1}{}^{A}$) are relatively high. Activation energy ($\Delta E_{a,TS1}{}^{A}$) for the reaction of SiH_3X and HCN decrease in the order X = H > Cl > Br > I with G3MP2 (B3LYP/6-31G(d,p) for X = I) activation energies of 280.7, 265.5, 261.1, and 256.0 kJ mol^{-1}, respectively.

The SiH_3CN/HX product can isomerize to form SiH_3NC/HX. The transition state structure (TS2^A) is a three-membered ring, consisting of C, N and SiH_3. The vibrational analysis shows the Si−N bond shortening and Si−C bond lengthening and vice versa. The activation energy ($\Delta E_{a,TS2}{}^{A}$) for the isomerization reaction is low compared to the elimination reaction and can proceed to form the SiH_3NC/HX complex. The barriers ($\Delta E_{a,TS2}{}^{A}$) for isomerization of SiH_3CN/HX to SiH_3NC/HX are 115.1, 121.2, and 119.7 kJ mol^{-1} at G3MP2 level for X = H, Cl and Br and 129.1 kJ mol^{-1} at B3LYP/6-31G(d,p) for X = I. The G3MP2 and G3B3 barriers differ by only 4.0 and 4.7 kJ mol^{-1} for X = H and Cl, respectively. The G3MP2 values are also found to be close to those obtained at B3LYP/6-31G(d,p) and differ by no more than 9.6 kJ mol^{-1} for HX elimination (X = H) and 10.6 kJ mol^{-1} for isomerization (X = Cl).

3.1.2. Reaction of SiH_3X and HCN (H_2 Elimination). There are four possible pathways for the H_2 elimination reaction:

$$SiH_3X + HCN \rightarrow SiH_2XCN + H_2, \quad X = H, Cl, Br, and I$$

The four pathways are designated as pathway B1 (one-step) and pathways B2, B3, and B4 (multiple steps). Pathways B2, B3, and B4 all lead to intermediate I1^{B*}, which proceeds to product via pathway B*. Reactants, intermediates, transition states, and products involved in the H_2 elimination reaction of SiH_3Cl with HCN are shown in Figures 3 and 4. Similar structures are also observed for the reaction of HCN with SiH_4, SiH_3Br, and SiH_3I and hence are not shown. The relative energies of reactants, intermediates, transition states, and products for pathways B1 and B* are shown in Figure 5. Similarly, the relative energies in pathways B2, B3, and B4 are shown in Figures 6, 7, and 8, respectively. Activation energies and free energies of activation for pathways B1, B*, and B2 are given in Table 2 and pathways B3 and B4 are given in Table 3.

Pathway B1 is a one-step mechanism in which a complex of SiH_2XCN and H_2 is formed via transition state TS1^{B1}, where

TABLE 9: Thermodynamic Properties for the Thermal Decomposition Reaction of SiH_3X (X = H, Cl, Br, I) (in kJ mol^{-1}) at 298.15 K[b]

	$SiH_4 \rightarrow SiH_2 + H_2$			$SiLH_3Cl \rightarrow SiHCl + H_2$		
level/basis set	Δ*E*	Δ*H*	Δ*G*	Δ*E*	Δ*H*	Δ*G*
HF/6-31G(d)	258.7	240.1	203.8	225.5	208.9	169.7
MP2/6-31G(d)	251.6	234.1	197.8	206.5	191.1	152.0
B3LYP/6-31G(d)	249.6	233.0	196.7	199.4	184.9	145.8
G3MP2	220.0	228.1	192.0	176.5	184.3	145.5
G3B3	223.9	232.0	195.8	181.8	189.6	150.6
		238.2[a]			196.4[a]	

	$SiH_3Br \rightarrow SiHBr + H_2$			$SiH_3I \rightarrow SiHI + H_2$		
level/basis set	Δ*E*	Δ*H*	Δ*G*	Δ*E*	Δ*H*	Δ*G*
HF/6-31G(d)	220.4 (223.5)	204.2 (207.0)	165.0 (167.8)	216.1	200.2	161.1
MP2/6-31G(d)	201.1 (203.3)	186.0 (187.9)	147.0 (148.8)	196.6	181.9	142.9
B3LYP/6-31G(d)	193.5 (196.6)	179.4 (182.2)	140.3 (143.1)	188.0	174.2	135.2
G3MP2	197.5 (197.5)	205.3 (205.3)	166.5 (169.3)			

further reactions

	$SiHCl + H_2 \rightarrow SiH_2 + HCl$			$SiHBr + H_2 \rightarrow SiH_2 + HBr$		
level/basis set	Δ*E*	Δ*H*	Δ*G*	Δ*E*	Δ*H*	Δ*G*
HF/6-31G(d)	99.2	101.2	97.4	98.8 (119.6)	99.2 (119.8)	95.4 (115.9)
MP2/6-31G(d)	133.7	135.2	131.4	137.4 (156.4)	137.4 (156.3)	133.5 (152.3)
B3LYP/6-31G(d)	121.4	122.3	118.6	122.2 (140.5)	121.6 (139.8)	118.0 (136.0)
G3MP2	123.6	122.9	119.3	100.2 (98.5)	99.2 (97.6)	95.6 (93.9)
G3B3	119.2	118.4	114.8			

	$SiHI + H_2 \rightarrow SiH_2 + HI$		
level/basis set	Δ*E*	Δ*H*	Δ*G*
HF/6-31G(d)	98.0	96.5	92.7
MP2/6-31G(d)	138.4	136.5	132.7
B3LYP/6-31G(d)	122.9	120.8	117.2

[a] The value is obtained from ref 23. [b] The values in parentheses are calculated by using the Binning−Curtiss bromine basis set from ref 39.

TABLE 10: Thermodynamic Properties for the Reaction of SiHX (X = H, Cl, Br, I) with HCN (in kJ mol^{-1}) at 298.15 K[a]

	$SiH_2 + HCN \rightarrow SiH_3CN$			$SiHCl + HCN \rightarrow SiH_2ClCN$		
level/basis set	Δ*E*	Δ*H*	Δ*G*	Δ*E*	Δ*H*	Δ*G*
HF/6-31G(d)	−261.1	−253.3	−209.7	−218.0	−213.5	−169.4
MP2/6-31G(d)	−280.1	−271.7	−228.6	−231.2	−225.9	−182.5
B3LYP/6-31G(d)	−265.0	−257.4	−214.2	−209.8	−205.2	−161.6
G3MP2	−255.7	−260.9	−218.2	−210.9	−214.9	−171.7
G3B3	−257.2	−262.5	−219.5	−213.8	−217.8	−174.5

	$SiHBr + HCN \rightarrow SiH_2BrCN$			$SiHI + HCN \rightarrow SiH_2ICN$		
level/basis set	Δ*E*	Δ*H*	Δ*G*	Δ*E*	Δ*H*	Δ*G*
HF/6-31G(d)	−211.1 (−217.1)	−206.9 (−212.8)	−162.8 (−168.8)	−205.2	−201.3	−157.2
MP2/6-31G(d)	−224.3 (−228.5)	−219.4 (−223.4)	−175.9 (−180.1)	−218.7	−214.0	−170.6
B3LYP/6-31G(d)	−202.5 (−208.5)	−198.2 (−204.2)	−154.7 (−160.7)	−195.9	−192.0	−148.5
G3MP2	−231.3 (−231.5)	−235.1 (−235.2)	−192.0 (−192.2)			

[a] The values in parentheses are calculated by using the Binning−Curtiss bromine basis set from ref 39.

the HCN carbon is attacking the Si and the hydrogen of HCN is simultaneously combining with a hydrogen of SiH_3X to form H_2. In $TS1^{B1}$, the Si−C bond distance decreases in the order X = H > Cl > Br > I, with the Si−C bond distances of 2.329, 2.223, 2.217, and 2.213 Å, respectively, at MP2/6-31G(d) level of theory. The ∠H−Si−H bond angle remain relatively constant for X = H, Cl, Br, and I with values of 30.0, 31.3, 31.4, and 31.5°, respectively, at MP2/6-31G(d) level of theory. The activation energies ($\Delta E_{a,TS1}{}^{B1}$) at G3MP2 for X = H, Cl, and Br are 280.7, 252.8, and 256.1 kJ mol^{-1}, respectively. For the reaction of HCN and SiH_3I, the activation energies at MP2/6-31G(d,p) and B3LYP/6-31G(d,p) are 296.8 and 272.0 kJ mol^{-1}, respectively. Activation energies obtained at G3MP2 and G3B3 levels are within 1.1 kJ mol^{-1} for the reactions of HCN with SiH_4 and SiH_3Cl. Also, for X = H, Cl, and Br, the activation energies obtained at B3LYP/6-31G(d,p) differ from the G3 values by no more than 10.9 kJ mol^{-1} (X = Cl, G3B3).

In pathway B2, intermediate $I1^{B*}$ is formed via $TS1^{B2}$ in a single-step, which involves a proton transfer from SiH_3X. The activation energies ($\Delta E_{a.TS1}{}^{B2}$) at G3MP2 are 265.4, 236.6, and 239.0 kJ mol^{-1} for X = H, Cl and Br, respectively. For X = I, the activation energy is 245.8 kJ mol^{-1} at B3LYP/6-31G(d,p). Pathway B3 is a three-step process, where intermediate $I1^{B3}$ is formed via $TS1^{B3}$, which also involves a proton transfer from SiH_3X. The activation energies ($\Delta E_{a,TS1}{}^{B3}$) are 268.6 and 271.0 kJ mol^{-1} at G3MP2 and 274.6 kJ mol^{-1} at B3LYP/6-31G(d,p) for X = Cl, Br, and I, respectively. Then intermediate $I2^{B3}$, a conformational isomer of $I1^{B3}$, is formed via $TS2^{B3}$, with activation energies of only 6.0 and 6.4 kJ mol^{-1} at G3MP2 and 11.0 kJ mol^{-1} at B3LYP/6-31G(d,p) for X = Cl, Br, and I,

TABLE 11: Heat of Formation (ΔH_f) (in kJ mol^{-1}) at 298.15 K

	experimental	present work		present work[a]
SiH_4	34.7[b]	35.8[j]	SiH_3CN	133.5 (134.6)[i]
HCN	131.67[c]		SiH_3NC	150.8
SiH_3Cl	−135.6[d]	−136.7[k]	SiH_2ClCN	−34.4
HCl	−92.21[e]	−91.1[k]	SiH_2BrCN	23.7
SiH_3Br	−78.24[f]	−78.0[k]	SiH_2ICN	102.4
HBr	−36.2[e]	−36.5[k]	SiHCl	48.7
SiH_3I	-2.09 ± 2[g]		SiHBr	127.1
HI	25.92[e]		SiHI	179.8
SiH_2	273.8 ± 4.2[h]	262.8[l]		

[a] See text for explanation. [b] References 42 and 43. [c] Reference 44. [d] Reference 45. [e] References 46 and 47. [f] Reference 43. [g] Reference 47. [h] Reference 48. [i] The value in parentheses is obtained by using the heat of reaction of $SiH_3Cl + HCN \rightarrow SiH_3CN + HCl$ and experimental ΔH_f of SiH_3Cl, HCN and HCl. [j] The value is obtained by using the heat of reaction of $SiH_4 + HCN \rightarrow SiH_3CN + H_2$ and $\Delta H_f(SiH_3CN) = 134.6$ kJ mol^{-1}. [k] The values are obtained by using the heat of reaction of $SiH_3X + HCN \rightarrow SiH_3CN + HX$ (X = Cl and Br) and experimental ΔH_f values for SiH_3X, HCN and HX and the calculated $\Delta H_f(SiH_3CN) = 133.5$ kJ mol^{-1}. [l] The value is obtained by using the heat of reaction of $SiH_4 \rightarrow SiH_2 + H_2$ and the experimental ΔH_f value for SiH_4.

respectively. Finally, intermediate $I1^{B*}$ is formed via $TS3^{B3}$, which involves rotation about the C−N bond. The activation energies ($\Delta E_{a,TS3}{}^{B3}$) are 176.5 and 176.0 kJ mol^{-1} at G3MP2 and 190.5 kJ mol^{-1} at B3LYP/6-31G(d,p) for X = Cl, Br, and I, respectively. Pathway B4 is a two-step process leading to intermediate $I1^{B*}$. First, intermediate $I1^{B4}$ is formed via $TS1^{B4}$, where a hydride shift occurs from SiH_3X, with activation energies of 260.7 and 261.4 kJ mol^{-1} at G3MP2 and 268.2 kJ mol^{-1} at B3LYP/6-31G(d,p) for X = Cl, Br, and I, respectively. Finally, the intermediate $I1^{B*}$ is formed via $TS2^{B4}$, which involves rotation about the Si−N bond, with very low activation energy (Table 3). Note that pathways B3 and B4 do not exist for X = H.

In pathway B*(Figures 3 and 5), a common pathway for B2, B3 and B4, intermediate $I1^{B*}$ eliminates H_2, (one H from the C atom and one from the N atom) via $TS1^{B*}$ to form a SiH_2XNC/H_2 complex. In the intermediate I1B*, the H−H bond distance for X = H, Cl, Br, and I are 2.253, 2.240, 2.235, and 2.550 Å, respectively, at MP2/6-31G(d) level of theory, while in $TS1^{B*}$, they decrease to 1.022, 1.035, 1.037, and 1.039 Å. The activation energies ($\Delta E_{a,TS1}{}^{B*}$) are 262.3, 258.7, and 256.4 kJ mol^{-1} at G3MP2 for X = H, Cl, and Br and the barrier ($\Delta E_{a,TS1}{}^{B*}$) for X = I is 297.4 kJ mol^{-1} at the B3LYP/6-31G(d,p) level. Finally, pathway B* is connected to pathway B1 by the isomerization of SiH_2XNC/H_2 via $TS2^{B*}$ with activation energies of 97.3, 107.2, and 106.2 kJ mol^{-1} at G3MP2 and 107.4 kJ mol^{-1} at B3LYP/6-31G(d,p) for X = H, Cl, Br, and I, respectively. Therefore, of the four pathways, B1, B2, B3, and B4, pathway B1 is the most energetically favorable. However, formation of a new intermediate $H_2XSi{-}NHCH$ ($I1^{B*}$) is possible via pathways B2, B3, and B4.

3.1.3. Decomposition of SiH_3X and Reaction with HCN. At elevated temperatures, SiH_4, SiH_3Cl, SiH_3Br and SiH_3I can dissociate to form various products:

$$SiH_3X \rightarrow SiHX + H_2 \rightarrow SiH_2 + HX, \quad X = H, Cl, Br, \text{and } I$$

It is well-known[23,24] that $SiH_4 \rightarrow SiH_2 + H_2$ is favored over $SiH_4 \rightarrow SiH_3 + H$ and $SiH_3Cl \rightarrow SiHCl + H_2$ is favored over $SiH_3Cl \rightarrow SiH_2 + HCl$. The pathway for the decomposition of SiH_4 and SiH_3Cl are shown in Figure 9. Structures similar to the SiH_3Cl decomposition are also observed for the decomposition of SiH_3Br and SiH_3I. The activation energies, activation enthalpies and free energies of activation for the decomposition of SiH_4, SiH_3Cl, SiH_3Br, and SiH_3I are given in Table 4. The activation energies for $SiH_3X \rightarrow SiHX + H_2$ at G3MP2 are 233.1, 257.6, and 252.3 kJ mol^{-1} for X = H, Cl and Br, respectively, and 267.3 kJ mol^{-1} for X = I at B3LYP/6-31G(d). The products of the dissociation, $SiHX + H_2$, can react further to form $SiH_2 + HX$, by a one-step process. The barriers for $SiHX + H_2 \rightarrow SiH_2 + HX$ are lower than the barriers for dissociation of SiH_3X (X = Cl, Br, and I). For X = Cl and Br, the barriers are 128.7 and 118.5 kJ mol^{-1} at the G3MP2 level and 108.7 kJ mol^{-1} for X = I at B3LYP/6-31G(d).

The dissociation products (SiH_2 and SiHX) can react with HCN by a one-step mechanism leading to SiH_3CN and SiH_2XCN, respectively,

$$SiHX + HCN \rightarrow SiH_2XCN, \quad X = H, Cl, Br, \text{and } I.$$

The transition state (TS3) involves one bond rupture (C−H) and two bond formations (Si−H and Si−C). The C−H bond distance of HCN in SiHX/HCN for X = H, Cl, Br, and I have a relatively constant value of 1.073 Å at MP2/6-31G(d)level of theory, which increase to 1.416, 1.478, 1.473, and 1.463 Å, respectively, in TS3. The Si−C bond distance in TS3 is almost constant (1.856 Å) for X = Cl, Br, and I, while for X = H, the Si−C bond distance is 1.868 Å at MP2/6-31G(d)level of theory. The activation energies, activation enthalpies and free energies of activation for the reaction of SiH_2 and SiHX (X = Cl, Br, I) with HCN are given in Table 5. The activation energies are found to be significantly lower, 152.7 kJ mol^{-1} ($\Delta E_{a,TS1}{}^{A}$ (X = I), B3LYP/6-31G(d)) to 255.9 kJ mol^{-1} ($\Delta E_{a,TS1}{}^{A}$ (X = H), G3MP2), than the activation energies of direct reactions between SiH_3X and HCN, $\Delta E_{a,TS1}{}^{A}$ and $\Delta E_{a,TS1}{}^{B1}$ (Tables 1 and 2). The G3MP2 and G3B3 values differ by no more than 4.5 kJ mol^{-1} (X = H) and the B3LYP/6-31G(d,p) values agree well with the G3 values, differing by no more than 17.3 kJ mol^{-1} (X = Cl,G3MP2). The barriers for the reaction $SiHX{+}HCN \rightarrow SiH_2XCN$ generally increase in the order X = H < Br < Cl < I, with values of 24.8, 90.5, and 92.4 kJ mol^{-1} at G3MP2, for X = H, Br, and Cl, respectively, and 107.0 kJ mol^{-1} at B3LYP/6-31G(d) for X = I. Thus, the formation of SiH_3CN is favored over the formation of SiH_2XCN.

3.1.4. Summary of Overall Reaction Mechanisms Investigated. The favored mechanism of the reaction of SiH_3X with HCN depends upon the substituent, X. For X = H, decomposition has the lowest barrier, 233 kJ mol^{-1} at the G3MP2 level, producing $SiH_2 + H_2$. Therefore, SiH_3CN could be formed from the reaction of SiH_2 and HCN, which has an activation energy of only 25 kJ mol^{-1} at the G3MP2 level. For X = Cl, the H_2 elimination reaction is slightly favored over the decomposition reaction by 5 kJ mol^{-1} at the G3MP2 level (Tables 2 and 4) and the decomposition reaction is slightly favored over the HCl elimination reaction by 8 kJ mol^{-1} at the G3MP2 level (Tables 1 and 4). For X = Br, the decomposition reaction is favored over H_2 elimination and HBr elimination by 4 and 9 kJ mol^{-1}, respectively, at the G3MP2 level (Tables 1, 2, and 4). The most likely mechanism of reaction for X = I, is HX elimination, with activation energy of 260 kJ mol^{-1} at the B3LYP/6-31G(d) level of theory, producing SiH_3CN and HI. The SiH_3I decomposition reaction could also form SiH_3CN, since the decomposition barrier is 267 kJ mol^{-1} at the B3LYP/6-31G(d) level of theory. Within the error limit for B3LYP/6-31G(d) level of theory, the formation of SiH_2ICN by the H_2 elimination reaction cannot be eliminated, since the activation energy is 287 kJ mol^{-1} at B3LYP/6-31G(d).

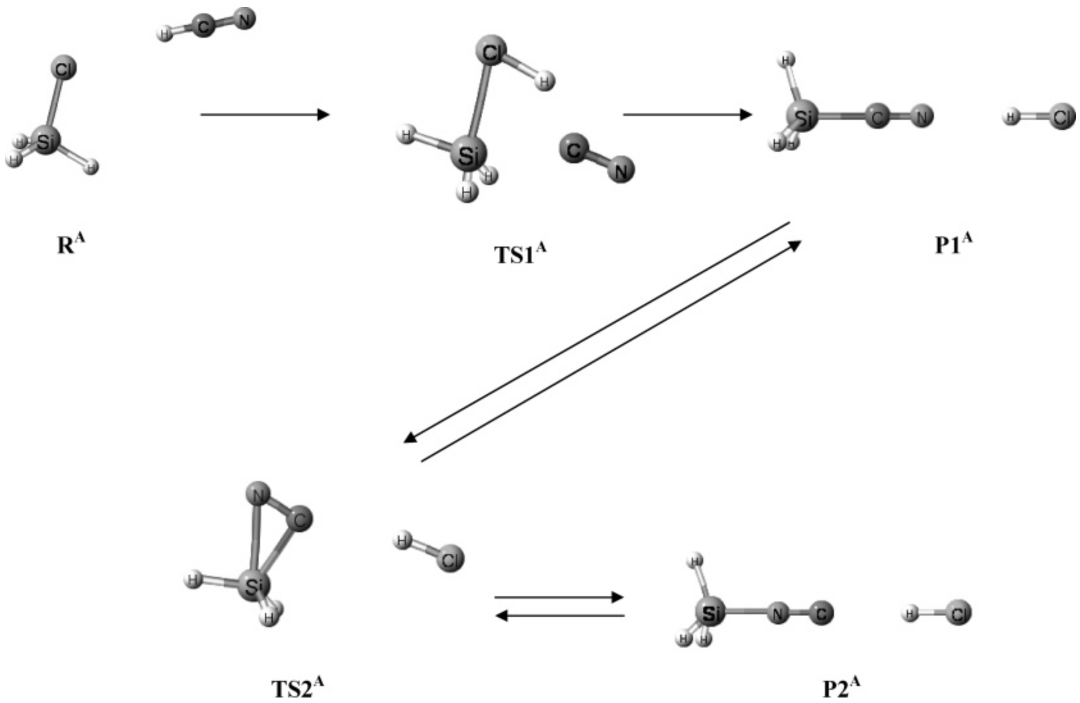

Figure 1. Mechanism for the reaction of $SiH_3X + HCN$ (pathway A). Only X = Cl is shown here, similar structures are found for X = Br and I.

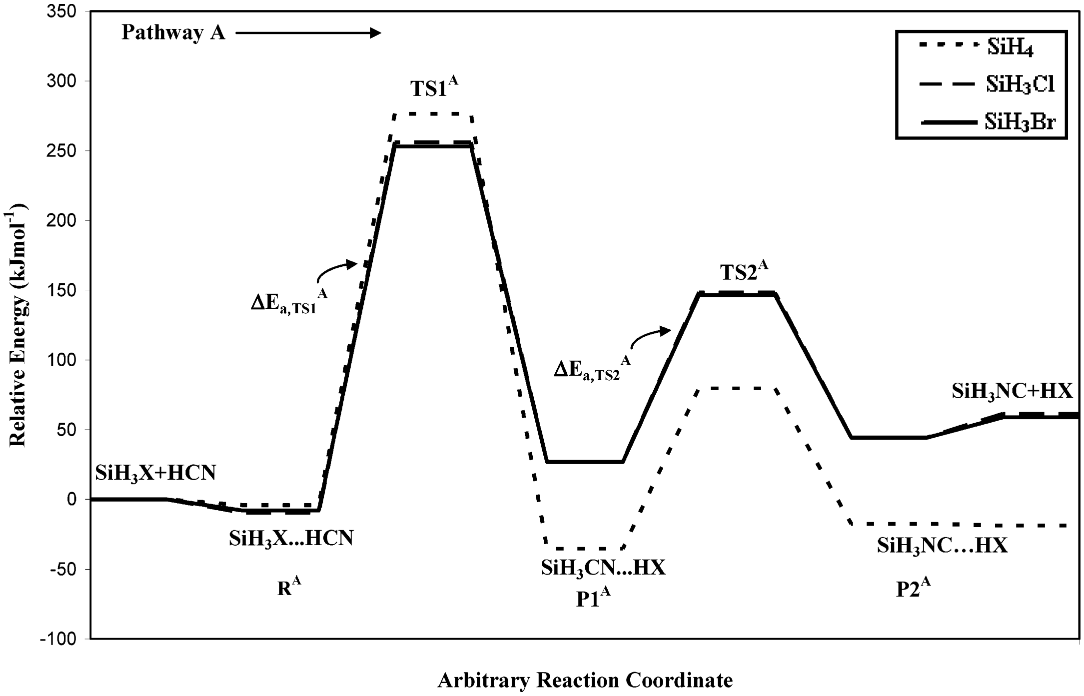

Figure 2. Reaction pathway for the reaction of $SiH_3X + HCN$ (pathway A) at G3MP2 level of theory (see Figure 1).

3.2. Thermodynamic Results for the Reaction of SiH_3X with HCN. *3.2.1. Thermodynamics of HX Elimination.* The thermodynamic properties of the reaction $SiH_3X + HCN \rightarrow SiH_3CN + HX$ (X = H, Cl, Br, I) are listed in Table 6. For X = H, the reaction is found to be exothermic for all levels of theory and basis set (with enthalpies of −32.9 and −30.5 kJ mol^{-1} at G3MP2 and G3B3, respectively). The MP2/6-31G(d,p) enthalpy is in better agreement with the G3 theories than the HF and B3LYP enthalpies. The free energies of reaction at G3MP2 and G3B3 are −26.2 and −23.7 kJ mol^{-1}, respectively. For X = Cl, Br, and I, the reactions are found to be endothermic for all levels of theory and basis set. For X = Cl and Br, the B3LYP/6-31G(d,p) enthalpies are in better agreement with the G3 theories than the HF and MP2 enthalpies. For X = Cl and Br, the enthalpies of reaction are 46.3 and 43.6 kJ mol^{-1} at G3MP2 and 33.9 kJ mol^{-1} at B3LYP/6-31G(d,p) for X = I. All the levels of theory predict the reaction to be endergonic. The free energies of reaction for X = Cl and Br, are 46.5 and 43.8 kJ mol^{-1} at G3MP2 and 34.6 kJ mol^{-1} at B3LYP/6-31G-(d,p) for X = I. For X = Br, the thermodynamic values obtained using Binning−Curtiss bromine basis set were found to be quite different compared to G3MP2 and all the other levels. However, the values obtained using recently developed 6-31G(d) bromine basis set[38] were found to agree very well with G3MP2 results.

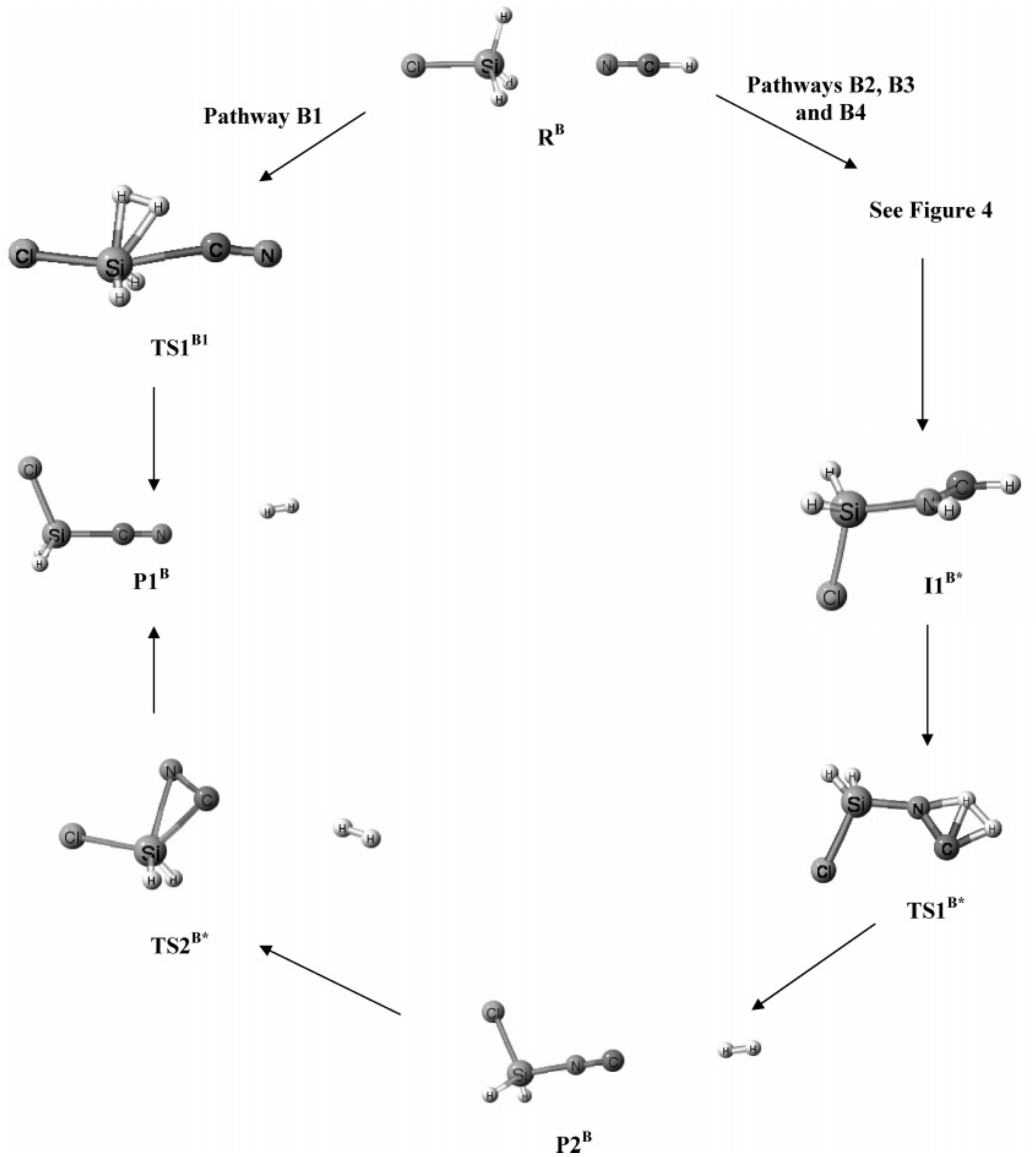

Figure 3. Mechanism for the reaction of $SiH_3X + HCN$ (H_2 elimination). Only X = Cl is shown here, similar structures are found for X = H, Br, and I.

The relative energies of the SiH_2XCN and SiH_2XNC isomers are given in Table 7. All levels of theory (except HF) predict the SiH_2XCN isomer to be more stable, with G3MP2 enthalpies of isomerization of 17.3, 9.8, 11.6 kJ mol^{-1}, for X = H, Cl, and Br, respectively and 20.4 kJ mol^{-1} for X = I at B3LYP/6-31G(d,p). The B3LYP/6-31G(d,p) enthalpies are consistently in better agreement with the G3 theories than the HF and MP2 enthalpies.

3.2.2. Thermodynamics of H_2 Elimination. The thermodynamic properties of the reaction $SiH_3X + HCN \rightarrow SiH_2XCN + H_2$ are listed in Table 8. The enthalpies of reaction for X = Cl and Br are −30.5 and −29.8 kJ mol^{-1} at G3MP2 and −27.2 and −17.6 kJ mol^{-1} at MP2/6-31G(d,p) and B3LYP/6-31G(d,p) for X = I. With the exception of HF/6-31G(d), all levels of theory predict the reactions to be exergonic. For X = Cl and Br, the free energies of reaction are −26.3 and −25.5 kJ mol^{-1} at G3MP2 level. For X = I, the free energy of reaction is −22.8 kJ mol^{-1} at MP2/6-31G(d,p) and −13.1 kJ mol^{-1} at B3LYP/6-31G(d,p). For both enthalpies and free energies of reaction, it is found that MP2/6-31G(d,p) values agree the best with G3 values.

3.2.3. Thermodynamics for the Thermal Decomposition of SiH_3X and $SiHX + HCN$. The thermodynamic properties for the decomposition of SiH_3X, X = H, Cl, Br, and I are given in Table 9. For all levels of theory and basis sets, the reactions are highly endothermic. The G3MP2 enthalpies of decomposition for X = H and Cl (228.1 and 184.3 kJ mol^{-1}) are found to agree well with previous calculations.[23] For X = Br, the G3MP2 enthalpy is 205.3 kJ mol^{-1} and 174.2 kJ mol^{-1} for X = I at B3LYP/6-31G(d). The subsequent reactions, $SiHX + H_2 \rightarrow SiH_2 + HX$ are also endothermic at all levels of theory. The decomposition reactions are all endergonic, with free energies of reaction for X = H, Cl, and Br of 192.0, 145.5, and 166.5 kJ mol^{-1} at G3MP2 and 135.2 kJ mol^{-1} for X = I at B3LYP/6-31G(d). The reaction of the dissociated products is found to be less endergonic, with free energies of reaction for X = Cl and

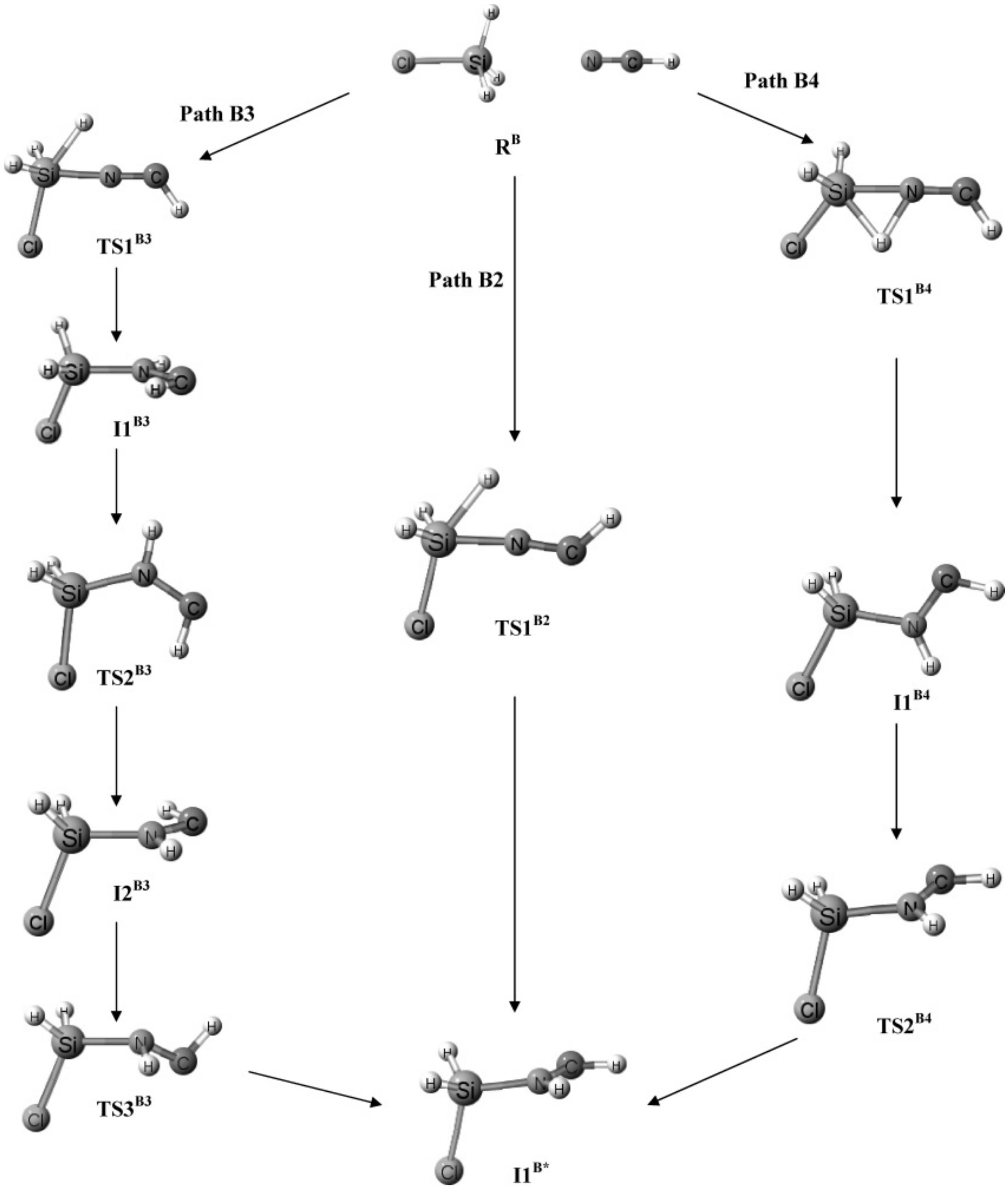

Figure 4. Mechanism for the reaction of $SiH_3X + HCN$ forming the intermediate $I1^{B*}$ (H_2 elimination). Only X = Cl is shown here; similar structures are found for X = H, Br, and I.

Br of 119.3, and 95.6 kJ mol^{-1} at G3MP2 and 117.2 kJ mol^{-1} for X = I at B3LYP/6-31G(d).

The products from thermal decomposition can also react with HCN. The reaction $SiH_2 + HCN \rightarrow SiH_3CN$ is found to be highly exothermic with enthalpies of reaction of −260.9 and −262.5 kJ mol^{-1} at G3MP2 and G3B3 respectively (Table 10). All the levels of theory also predict the reaction to be exergonic (−218.2 kJ mol^{-1} at G3MP2). Similar results are seen for the reactions $SiHX + HCN \rightarrow SiH_2XCN$. For X = Cl and Br, the free energies of reaction are −171.7, and −192.0 kJ mol^{-1} at G3MP2 and −148.5 kJ mol^{-1} at B3LYP/6-31G(d) for X = I. These reactions are less exergonic than the reaction of SiH_2 and HCN. Hence, formation of SiH_3CN is favored over formation of SiH_2XCN from the decomposition reaction pathway of SiH_3X and HCN.

3.3. Performance of Theory/Basis Set. All the reactions studied in this work are isogyric. When the HF results are compared with other levels of theory, it is evident that electron correlation is quite important in these reactions. For both kinetics and thermodynamics, the G3MP2 and G3B3 theories differ by no more than 6.7 kJ mol^{-1} for activation energies (X = H, $\Delta E_{a,TS1}{}^{B2}$) and 5.3 kJ mol^{-1} for reaction enthalpies and free energies (ΔH of $SiH_3Cl \rightarrow SiHCl + H_2$). However, for the lower levels of theory, performance depends on the reaction type. Compared to MP2, activation energies calculated using B3LYP consistently agree better with the G3 values. Barriers predicted by both B3LYP and MP2 are always larger than the G3 values, except for the isomerization step in pathway B*, $\Delta E_{a,\ TS2}{}^{B*}$ (Table 2), where the MP2 values are lower. For all reactions with X = Br, activation energies calculated using the standard 6-31G(d) bromine basis set do not differ by more than 10.1 kJ mol^{-1} (G3MP2, HX elimination reaction) compared to the Binning−Curtiss basis set results.

Thermodynamic values calculated using B3LYP and MP2 levels of theory are more comparable. For the majority of cases, B3LYP provides reaction enthalpies and free energies that are

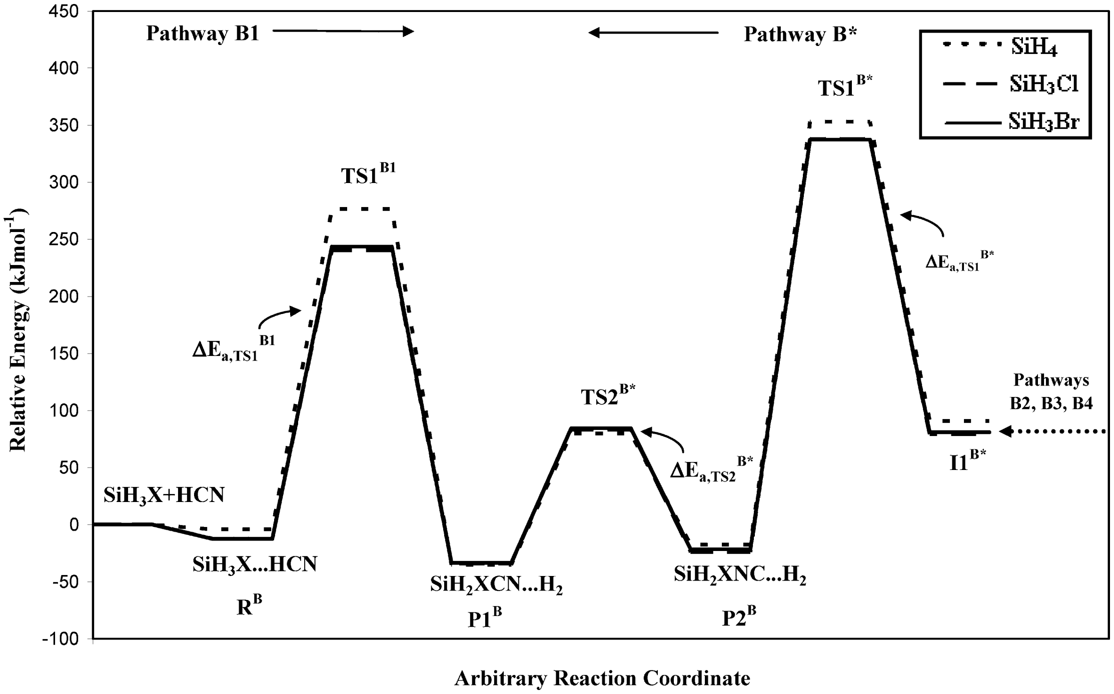

Figure 5. Reaction pathway B1 and B* for the reaction of SiH_3X + HCN (H_2 elimination) at G3MP2 level of theory (see Figure 3).

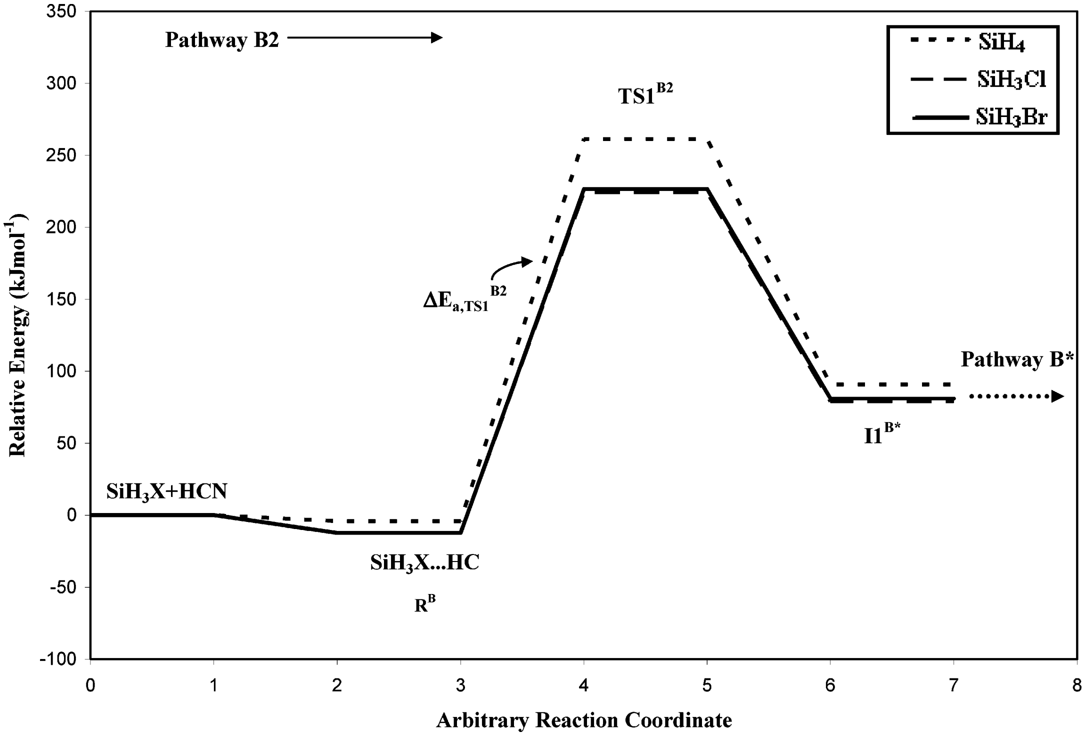

Figure 6. Reaction pathway B2 for the reaction of SiH_3X + HCN (H_2 elimination) at G3MP2 level of theory (see Figure 4).

in better agreement with G3 values. However, MP2 gives better results for the H_2 elimination reactions (and HX elimination reaction, X = H) (Tables 6 and 8). The enthalpies and free energies of reaction calculated using MP2 are also in better agreement with G3 values for the decomposition of SiH_3Br (Table 9) and the reaction SiHBr + HCN → SiH_2BrCN (Table 10). Thermodynamic values determined using HF theory do not agree with G3 theories as well as MP2 and B3LYP. HF performs very poorly on the isomerization (Table 7) and H_2 elimination reactions (Table 8). However, HF does perform well on the reactions of the SiHX +HCN → SiH_2XCN (Tables 10). Unlike kinetics, the thermodynamics for some of the reactions change significantly with the change of bromine basis set. For HBr elimination, the enthalpies and free energies of reaction differ by 17−24 kJ mol^{-1} at HF, MP2 and B3LYP level of theory with a change of bromine basis set. Similarly for SiHBr + H_2 → SiH_2 +HBr, the enthalpies and free energies of reaction differ by 18−20 kJ mol^{-1} at HF, MP2 and B3LYP level of theory. In all cases, the results with the standard 6-31G(d) bromine basis set are closer to the G3MP2 results.

Most barriers were lowered by the addition of p-polarization functions to hydrogen, due to the involvement of hydrogen atoms in the transition states, but had little effect on thermodynamic values. There was little to no effect on the barriers in

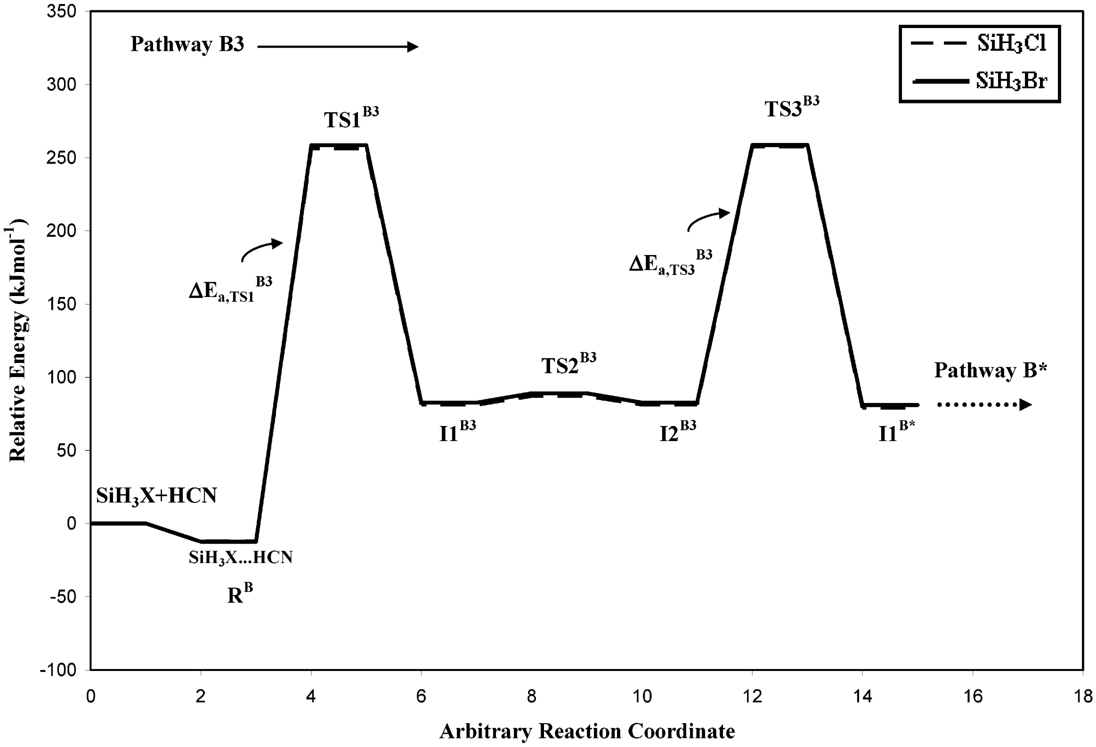

Figure 7. Reaction pathway B3 for the reaction of $SiH_3X + HCN$ (H_2 elimination) at G3MP2 level of theory (see Figure 4).

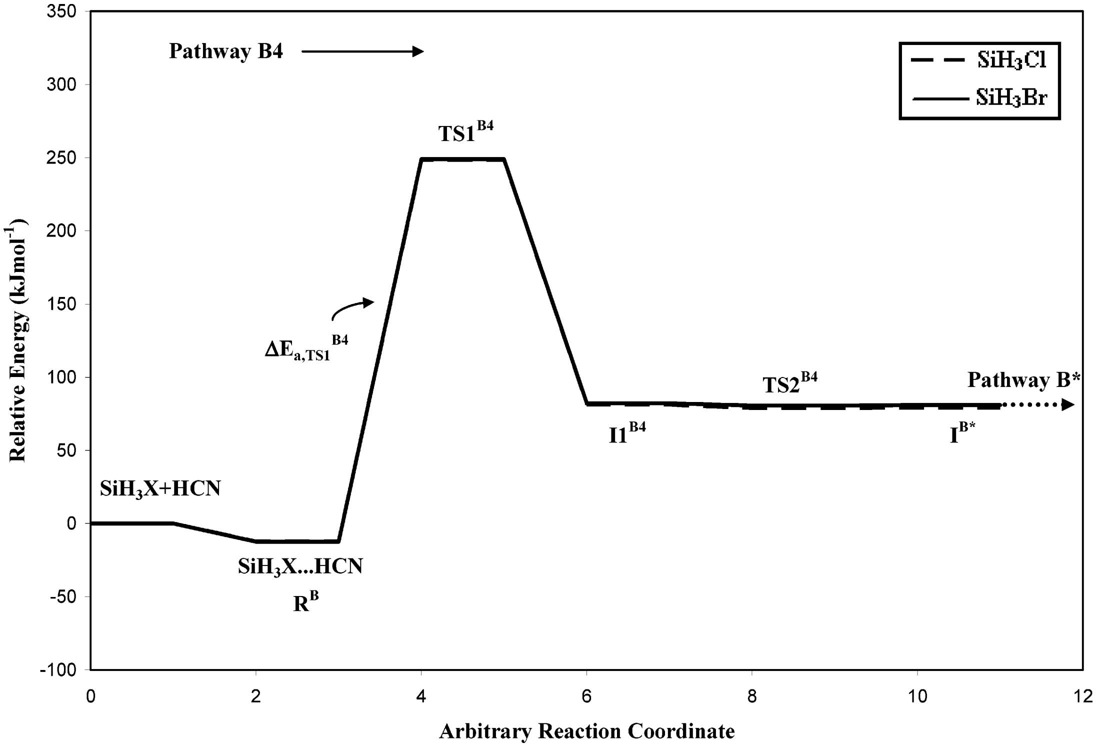

Figure 8. Reaction pathway B4 for the reaction of $SiH_3X + HCN$ (H_2 elimination) at G3MP2 level of theory (see Figure 4).

which hydrogen atoms were not directly involved in the transition states, such as $\Delta E_{a,TS2}{}^{A}$ (Table 1) and $\Delta E_{a,TS2}{}^{B*}$ (Table 2).

3.4. Exploring Heats of Formation (ΔH_f). No experimental or theoretical heats of formation (ΔH_f) have been reported for SiH_3CN and SiH_3NC. Part of this is due to the difficulty of carrying out such an experiment. In this study, the enthalpies of reaction for reactions between SiH_3X and HCN have been obtained. From this data, it is possible to calculate heats of formation for SiH_3CN, SiH_3NC, SiH_2ClCN, SiH_2BrCN, SiH_2ICN, SiH_2, SiHCl, SiHBr, and SiHI at a high level of theory. The ΔH_f values obtained in this study are given in Table 11. From the G3MP2 enthalpy of reaction of $SiH_4 + HCN \rightarrow SiH_3CN + H_2$ and the most recent and reliable experimental heats of formation for SiH_4 and HCN (given in Table 11), ΔH_f for SiH_3CN is calculated to be 133.5 kJ mol^{-1}. The ΔH_f for SiH_3CN can also be calculated using the G3MP2 enthalpy of reaction of $SiH_3Cl + HCN \rightarrow SiH_3CN + HCl$ and most recent experimental heats of formation for SiH_3Cl, HCN and HCl (given in Table 11). The resulting ΔH_f is 134.5 kJ mol^{-1}, both

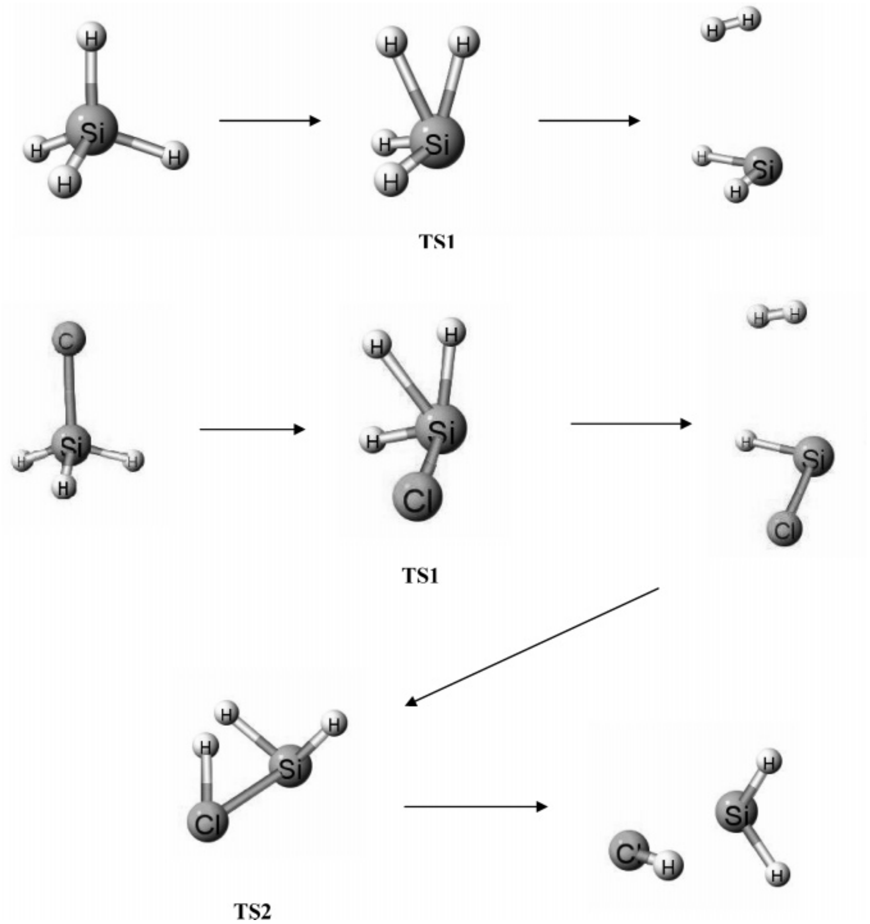

Figure 9. Mechanism for thermal decomposition of SiH_3X. Only X = H and Cl are shown here, similar structures to X = Cl are found for X = Br and I.

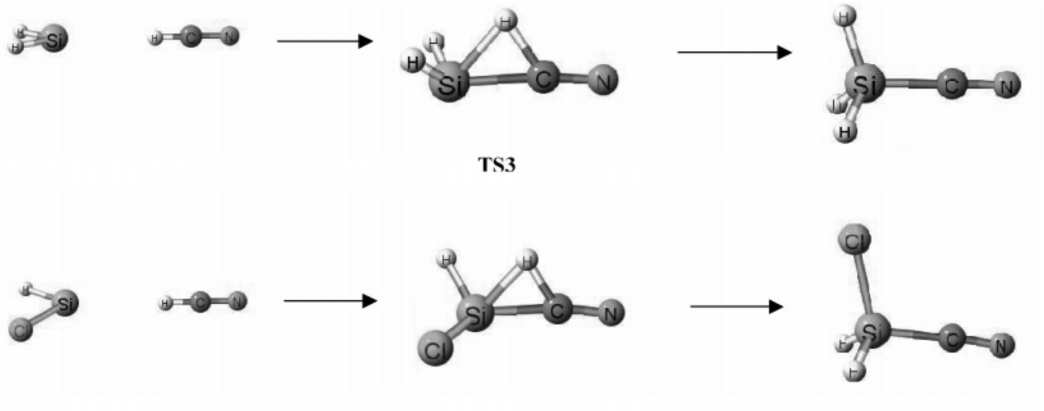

Figure 10. Mechanism for the addition reaction of SiHX + HCN. Only X = Cl are shown here, similar structures are found for X = H, Br, and I.

values being in excellent agreement. However, since the experimental heat of formation for SiH_4 is more reliable, the heat of formation of SiH_3CN calculated using the first reaction is most likely more reliable. Similarly, ΔH_f for SiH_3NC (150.8 kJ mol^{-1}) is obtained by using the G3MP2 enthalpy of isomerization for SiH_3CN to SiH_3NC (Table 7) and the calculated ΔH_f for SiH_3CN (133.5 kJ mol^{-1}). Heats of formation of SiH_2ClCN, SiH_2BrCN and SiH_2ICN are calculated using the enthalpies of reaction for $SiH_3Cl + HCN \rightarrow SiH_2ClCN + H_2$ (−30.5 kJ mol^{-1} at G3MP2), $SiH_3Br + HCN \rightarrow SiH_2BrCN + H_2$ (−29.8 kJ mol^{-1} at G3MP2) and $SiH_3I + HCN \rightarrow SiH_2ICN + H_2$ (−17.6 kJ mol^{-1} at B3LYP/6-31G(d,p)), along with experimental heats of formation for SiH_3Cl, SiH_3Br, SiH_3I and HCN (given in Table 11). The ΔH_f for SiHX (X = Cl, Br, I) can be calculated using G3MP2 enthalpies of reaction from both the $SiH_3X \rightarrow SiHX + H_2$ reaction and the $SiHX + H_2 \rightarrow SiH_2 + HX$ reaction (Table 9), along with experimental ΔH_f for SiH_3Cl, SiH_3Br, SiH_3I, SiH_2, HCl, HBr, and HI obtained from the literature (Table 11). Schlegel et al.[41] obtained a ΔH_f for SiHCl of 62.8 kJ mol^{-1} compared to 48.7 (54.0) and 58.7 (63.2) kJ mol^{-1} obtained from the G3MP2 (G3B3) enthalpies of reaction for $SiH_3Cl \rightarrow SiHCl + H_2$ and $SiHCl + H_2 \rightarrow SiH_2 + HCl$, respectively. The ΔH_f of 48.7 kJ mol^{-1} is recommended for SiHCl, since only $\Delta H_f(SiH_3Cl)$ and ΔH_{rxn} are required. The ΔH_f-

(SiHBr) values obtained by using $SiH_3Br \rightarrow SiHBr + H_2$ and $SiHBr + H_2 \rightarrow SiH_2 + HBr$ are found to be 127.1 and 138.4 kJ mol^{-1}, respectively; while ΔH_f(SiHI) is found to be 179.8 and 178.9 kJ mol^{-1}, using $SiH_3I \rightarrow SiHI + H_2$ and $SiHI + H_2 \rightarrow SiH_2 + HI$, respectively. Heats of formation calculated using $SiH_3X \rightarrow SiHX + H_2$ are considered more reliable because only one experimental ΔH_f is required. Heats of formation were also calculated, where possible, for SiH_4, SiH_3Cl, HCl, SiH_3Br, HBr, and SiH_2, for which experimental ΔH_f values are available for comparison. All the ΔH_f values are in excellent agreement with the experimental values except for the ΔH_f value for SiH_2, where the calculated $\Delta H_f(SiH_2)$ is found to be 262.8 kJ mol^{-1} compared to the experimental values of 273.8 ± 4.2 kJ mol^{-1}.

4. Conclusions

Three possible mechanisms of reaction between SiH_3X and HCN have been investigated: HX elimination, H_2 elimination, and reaction of HCN with SiH_3X dissociation products. Reaction via H_2 elimination can involve several different pathways, and HCN can also react with the decomposition products of SiH_3X. The activation energies for the rate-determining step of each mechanism suggest that for $X = H$, the decomposition mechanism ($SiH_4 \rightarrow SiH_2 + H_2$) is preferred and in this case SiH_3CN can be formed by reaction of SiH_2 with HCN. For $X = Cl$, H_2 elimination ($SiH_3Cl + HCN \rightarrow SiH_2ClCN + H_2$) is slightly favored where as for $X = Br$, the decomposition reaction ($SiH_3Br \rightarrow SiHBr + H_2 \rightarrow SiH_2 + HBr$) is favored. For $X = I$, mainly SiH_3CN product could be formed via HX elimination reaction ($SiH_3I + HCN \rightarrow SiH_3CN + HI$) and decomposition reaction ($SiH_3I \rightarrow SiHI + H_2 \rightarrow SIH_2 + HI$). When considering thermodynamics, it is noticed that the HX elimination reaction is endothermic and endergonic, except for $X = H$, while the H_2 elimination reaction is exothermic and exergonic for all X.

For both kinetics and thermodynamics, the G3 theories are generally in good agreement ($X = H$ and Cl). Values calculated using MP2 or B3LYP levels of theory are generally in better agreement with G3 theories than HF values. For the reactions studied here, B3LYP/6-31G(d,p) gives barriers similar to G3 values and MP2/6-31G(d,p) gives the best results for thermodynamics with the exception of the dissociation reactions. The kinetic and thermodynamic values obtained by using the standard 6-31G(d) bromine basis set are in much better agreement with the G3MP2 values compared to those obtained using Binning−Curtiss bromine basis set. Therefore, we recommend that the standard 6-31G(d) bromine basis set be used for calculations involving bromine.

It has also been shown that the reaction enthalpies, along with existing experimental data can be used to calculate heats of formation, which are otherwise unknown. Since high level calculations, such as G3MP2 and G3B3, are used to calculate reaction enthalpies, relatively good estimates of heats of formation are obtained.

Acknowledgment. We would like to thank the Natural Sciences and Engineering Council of Canada (NSERC) for financial support and gratefully acknowledge the Memorial University of Newfoundland Advanced Computation and Visualization Centre and the Atlantic Computational Excellence Network (ACEnet) for computer time.

Supporting Information Available: Tables of full geometries and energies of all structures for the reaction of SiH_3X with HCN. This material is available free of charge via the Internet at http://pubs.acs.org.

References and Notes

(1) Gershevitz, O.; Sukenik, C. N.; Ghabboun, J.; Cahen, D. *J. Am. Chem. Soc.* **2003**, *125*, 4730.

(2) Koinuma, H.; Manako, T.; Natsuaki, H.; Fujioka, H.; Fueki, K. *J. Non-Cryst. Solids* **1985**, *77*, 801.

(3) Matsuda, A.; Yagii, K.; Kaga, T.; Tanaka, K. *Jpn. J. Appl. Phys.* **1984**, *23*, 576.

(4) Sato, K.; Hirano, T.; Natsuaki, H.; Fueki, K.; Koinuma, H. *Appl. Phys. Lett.* **1984**, *45*, 1324.

(5) Hu, S.; Wang, Y.; Wang, X.; Chu, T.; Liu, X. *J. Phys. Chem. A* **2003**, *107*, 9189.

(6) Hu, S.; Wang, Y.; Wang, X.; Chu, T.; Liu, X. *J. Phys. Chem. A* **2004**, *108*, 1448.

(7) McCarthy, M. C.; Gottlieb, C. A.; Thaddeus, P. *Mol. Phys.* **2003**, *101*, 697.

(8) Stannowski, B.; Rath, J. K.; Schropp, R. E. *J. Appl. Phys.* **2003**, *93*, 2618.

(9) Patil, S. B.; Kumbha, A.; Waghmare, P.; Rao, V. R.; Dusane, R. O. *Thin Solid Films* **2001**, *395*, 270.

(10) Boehme, C.; Lucovsky, G. *J. Vac. Sci. Technol. A* **2001**, *19*, 2622.

(11) Gleskova, H.; Wagner, S.; Gasparik, V.; Kovac, P. *Appl. Surf. Sci.* **2001**, *175*, 12.

(12) Santana, G.; Morales-Acevedo, A. *Sol. Energ. Mat. Sol. C* **2000**, *60*, 135.

(13) Ghosh, S.; Dutta, P. K.; Bose, D. N. *Mater. Sci. Semicond. Proc.* **1999**, *2*, 1.

(14) Sahu, S.; Kavecky, S.; Szepvolgyi, J. *J. Eur. Ceram. Soc.* **1995**, *15*, 1071.

(15) Du, Z. D.; Chen, J. H.; Bei, X. L.; Zhou, C. G. *Organosilicon Chemistry*; Advanced Education Press: Beijing, 1990; p 80.

(16) Du, Z. D.; Chen, J. H.; Bei, X. L.; Zhou, C. G. *Organosilicon Chemistry*; Advanced Education Press: Beijing, 1990; p 101.

(17) Burg, A. B. *J. Am. Chem. Soc.* **1954**, *76*, 2654.

(18) Campbell-Ferguson, H. J.; Ebsworth, E. A. V. *Chem. Ind.* **1965**, 301.

(19) Aylett, B. J.; Sinclair, R. A. *Chem. Ind.* **1965**, 301.

(20) Aylett, B. J.; Emeleus, H. J.; Maddock, A. G. *J. Inorg. Nucl. Chem.* **1955**, *1*, 187.

(21) Campbell-Ferguson, H. J.; Ebsworth, E. A. V. *J. Chem. Soc. A* **1966**, 1508.

(22) Feng, S.; Feng, D.; Li, M.; Zhao, Y.; Wang, P. G. *J. Mol. Struct.* **2002**, *618*, 51.

(23) Su, M.; Schlegel, H. B. *J. Phys. Chem.* **1993**, *97*, 9981.

(24) Gordon, M. S.; Schlegel, H. B.; Francisco, J. S. Reaction Energetics in Silicon Chemistry. *Adv. Silicon Chem.* **1993**, *2*, 137.

(25) Pacheco-Sanchez, J. H. P.; Luna-Garcia, H.; Castillo, S. *J. Chem. Phys.* **2004**, *121*, 5777.

(26) Guelin, M.; Muller, S.; Cernicharo, J.; Apponi, A. J.; McCarthy, M. C.; Gottlieb, C. A.; Thaddeus, P. *Astron. Astrophys.* **2000**, *363*, L9.

(27) Sanz, E. M.; McCarthy, M. C.; Thaddeus, P. *Astrophys. J.* **2002**, *577*, 71.

(28) Apponi, A. J.; McCarthy, M. C.; Gottlieb, C. A.; Thaddeus, P. *Astrophys. J.* **2000**, *536*, L55.

(29) Maier, G.; Reisenauer, H. P.; Egenolf, H.; Glatthaar, J. *Eur. J. Org. Chem.* **1998**, 1307.

(30) Wang, Q.; Ding, Y.; Sun, C. *J. Phys. Chem. A* **2004**, *108*, 10602.

(31) Curtiss, L. A.; Redfern, P.C.; Raghavachari, K.; Rassolov, V.; Pople, J. A. *J. Chem. Phys.* **1999**, *110*, 4703.

(32) Baboul, A. G.; Curtiss, L. A, Redfern, P. C.; Raghavachari, K. *J. Chem. Phys.* **1999**, *110*, 7650.

(33) GAUSSIAN03, Revision A. 9, Gaussian Inc.: Pittsburgh, PA, 2003.

(34) Poirier, R. A. MUNgauss (Fortran 90 version), Chemistry Department, Memorial University of Newfoundland, St. John's, NL, A1B 3X7. With contributions from Bungay, S. D.; El-Sherbiny, A.; Gosse, T.; Hollett, J.; Keefe, D.; Kelly, A.; Pye, C. C.; Reid, D.; Shaw, M.; Wang, Y.; Xidos, J.

(35) Almatarneh, M. H.; Flinn, C. G.; Poirier, R. A. *Can. J. Chem.* **2005**, *83*, 2082.

(36) Curtiss, L. A.; Redfern, P. C.; Rassolov, V.; Kedziora, G. S.; Pople, J. A. *J. Chem. Phys.* **2001**, *114*, 9287.

(37) http://chemistry.anl.gov/compmat/comptherm.htm.

(38) Rassolov, V. A.; Ratner, M. A.; Pople, J. A.; Redfern, P. C.; Curtiss, L. A. *J. Comput. Chem.* **2001**, *22*, 976−984.

(39) Binning, R. C., Jr.; Curtiss, L. A. *J. Comput. Chem.* **1990**, *11*, 1206.

(40) Andzelm, J.; Klobukowski, M.; Radzio-andzelm, E.; Sakai, Y.; Tatewaki, H. In *Physical Sciences Data 16 Gaussian Basis Sets for Molecular Calculations*; Huzinaga, S., Ed.; Elsevier Science Publishers: Amsterdam, 1984; p 295.

(41) Su, M.; Schlegel, H. B. *J. Phys. Chem.* **1993**, *97*, 8732.

(42) Gurvich, L. V.; Veyts, I. V.; Alcock, C. B. *Thermodynamic Properties of Individual Substances*; Hemisphere: New York, 1991; Vol. 2, Part I.

(43) Chase, M. W. *NIST-JANAF Thermochemical Tables*, 4th ed., Monograph 9. *J. Phys. Chem. Ref. Data* **1998**, 1−1951.

(44) Hansel, A.; Scheiring, C.; Glantschnig, M.; Lindinger, W. *J. Chem. Phys.* **1998**, *109*, 1748.

(45) Farber, M.; Srivastava, R. D. *J. Chem. Therm.* **1979**, *11*, 939.

(46) *CRC Handbook of Chemistry and Physics*; CRC: Boca Raton, FL, 1977−1978; Vol. 58.

(47) McBride, B. J.; Zehe, M. J.; Gordon, S. *NASA Glenn Coefficients for Calculating Thermodynamic Properties of Individual Species*; Glenn Research Center: Cleveland, OH, 2002.

(48) Moffat, H. F.; Jensen, K. F.; Carr, R. W. *J. Phys. Chem.* **1991**, *95*, 145.